

## FAST EVENTS IN SINGLE-CHANNEL CURRENTS ACTIVATED BY ACETYLCHOLINE AND ITS ANALOGUES AT THE FROG MUSCLE END-PLATE

By D. COLQUHOUN AND B. SAKMANN

*From the M.R.C. Receptor Mechanisms Research Group, Department of Pharmacology, University College London, Gower Street, London WC1E 6BT and the Max Planck Institut für biophysikalische Chemie, Postfach 2481, D3400 Göttingen, F.R.G.*

(Received 21 March 1985)

### SUMMARY

1. The fine structure of ion-channel activations by junctional nicotinic receptors in adult frog muscle fibres has been investigated. The agonists used were acetylcholine (ACh), carbachol (CCh), suberyldicholine (SubCh) and decan-1,10-dicarboxylic acid dicholine ester (DecCh).

2. Individual activations (bursts) were interrupted by short closed periods; the distribution of their durations showed a major fast component ('short gaps') and a minor slower component ('intermediate gaps').

3. The mean duration of both short and intermediate gaps was dependent on the nature of the agonist. For short gaps the mean durations ( $\mu$ s) were: ACh, 20; SubCh, 43; DecCh, 71; CCh, 13. The mean number of short gaps per burst were: ACh, 1.9; SubCh, 4.1; DecCh, 2.0.

4. The mean number of short gaps per burst, and the mean number per unit open time, were dependent on the nature of the agonist, but showed little dependence on agonist concentration or membrane potential for ACh, SubCh and DecCh.

5. The short gaps in CCh increased in frequency with agonist concentration and were mainly produced by channel blockages by CCh itself.

6. Partially open channels (subconductance states) were clearly resolved rarely (0.4% of gaps within bursts) but regularly. Conductances of 18% (most commonly) and 71% of the main value were found. However, most short gaps were probably full closures.

7. The distribution of burst lengths had two components. The faster component represented mainly isolated short openings that were much more common at low agonist concentrations. The slower component represented bursts of longer openings. Except at very low concentrations more than 85% of activations were of this type, which corresponds to the 'channel lifetime' found by noise analysis.

8. The frequency of channel openings increased slightly with hyperpolarization.

9. The short gaps during activations were little affected when (a) the  $[H^+]$ <sub>o</sub> or  $[Ca^{2+}]_o$  were reduced to 1/10th of normal, (b) when extracellular  $Ca^{2+}$  was replaced by  $Mg^{2+}$ , (c) when the  $[Cl^-]_i$  was raised or (d) when, in one experiment on an isolated inside-out patch, the normal intracellular constituents were replaced by KCl.

10. Reduction of  $[Ca^{2+}]_o$  to 1/10th of normal increased the single-channel conductance by 50%, and considerably increased the number of intermediate gaps.

11. No temporal asymmetry was detectable in the bursts of openings. Positive correlations were found between the lengths of successive apparent open times at low SubCh concentrations, but no correlations between burst lengths were detectable.

12. The component of brief openings behaves, at low concentrations, as though it originates from openings of singly occupied channels. However, the persistence of about 10% of brief openings at high concentrations makes it unlikely that this is the only mechanism.

13. Short gaps within bursts behave in our preparation in a way that is consistent with the view that they originate from multiple openings of the doubly occupied channel, before dissociation occurs. The evidence for this interpretation is circumstantial, and the results are consistent with other mechanisms too. However, the values for opening ( $\beta$ ) and dissociation ( $k_{-2}$ ) rate constants implied by this interpretation are consistent with the relative potencies of the agonists, the results of high concentration experiments, and, in the case of ACh, the phenomena of synaptic transmission. For ACh we find  $\beta = 30600 \text{ s}^{-1}$  and  $k_{-2} = 8150 \text{ s}^{-1}$ ; the mean length of a single opening (at  $-130 \text{ mV}$ ) was  $1/\alpha = 1.4 \text{ ms}$  (about one-third of the burst length), so the conformational equilibrium constant was  $\beta/\alpha = 43$ , and the equilibrium constant for binding was about  $80 \mu\text{M}$ . The values are inconsistent with the hypothesis that binding is much faster than channel opening. The results suggest that ACh has a higher efficacy but a lower affinity than SubCh.

#### INTRODUCTION

Until recently the measurement of currents through single ion channels activated by acetylcholine-like agonists in frog muscle end-plates had revealed little information about mechanisms that had not already been inferred from analysis of noise (Katz & Miledi, 1972; Anderson & Stevens, 1973). However, several new phenomena have now been observed. It has been found that single 'openings' of the ion channel are actually interrupted by brief closed periods (the *nachschlag* phenomenon) and that the number of very brief openings observed was greater than expected (Colquhoun & Sakmann, 1981); in addition, occasional channel currents (*sublevels*) were seen that were of smaller amplitude than the usual (full) open-channel current (Colquhoun & Sakmann, 1983). Qualitatively similar observations have been made on a number of other preparations, and with several different neurotransmitters; for example Cull-Candy & Parker (1982) who worked with glutamate and its analogues on locust muscle fibres, and Dionne & Leibowitz (1982) with acetylcholine-like agonists on snake muscle fibres. Similar phenomena have been observed with several cultured cell types (Hamill & Sakmann, 1981; Jackson, Lecar, Askanas & Engel, 1982; Jackson, Wong, Morris, Lecar & Christian, 1983; Auerbach & Sachs, 1983, 1984; Sine & Steinbach, 1984a, 1986).

These phenomena are mostly so rapid that their accurate measurement needs the best resolution that can be obtained. It is our purpose in this paper to present measurements with several acetylcholine-like agonists on junctional nicotinic receptors of frog muscle fibres, to describe the observed phenomena in as much detail as

possible, and to discuss the possible interpretations of the results in terms of the mechanism of action of the transmitter.

## METHODS

### *The preparation*

Frogs (*Rana temporaria*) were used in all experiments. To obtain single fibres with their end-plates exposed the enzyme treatment described by Hamill, Marty, Neher, Sakmann & Sigworth (1981) was used. The end-plate region was observed at a magnification of 256 in a Zeiss microscope with a  $\times 16$  objective using Normarski interference contrast. All recordings were made with the pipette tip placed either in the synaptic trough or less than  $10\text{ }\mu\text{m}$  away from it, on perijunctional membrane. All recordings were made from the junctional type of channel (extrajunctional channels were seen very rarely). The appearance of the end-plate region of a living fibre as seen during the experiment is shown in Pl. 1.

### *Solutions*

All recordings were made with muscles bathed in standard frog Ringer solution of the following composition (mm): NaCl, 115; KCl, 2.5; CaCl<sub>2</sub>, 1.8; Na<sub>2</sub>HPO<sub>4</sub>, 2.15; NaH<sub>2</sub>PO<sub>4</sub>, 0.5; pH 7.2, 228 mosm. All experiments were carried out at a temperature of 10.5–11.5 °C. In all experiments except in those where the effect of ion composition was tested, the patch pipette contained a solution with the following composition (mm): NaCl, 115; KCl, 2.5; CaCl<sub>2</sub>, 1.8; HEPES, 5. To change the pH from 7.2 to 8.2 the HEPES buffer was titrated with NaOH. To change [Ca<sup>2+</sup>] the nominal concentration of CaCl<sub>2</sub> was reduced from 1.8 to 0.18 mm. Acetylcholine chloride (ACh) and carbamylcholine chloride (CCh) were obtained from Sigma. Suberyldicholine iodide (SubCh), and its longer chain analogue, the dicholine ester of decan-1,10-dicarboxylic acid (DecCh) were synthesized by J. Heeseman (Heeseman, 1981). All solutions contained tetrodotoxin (Sigma) at a concentration of 0.5–1 μM.

### *Single-channel measurements*

Preparations usually were viable for two days following the dissection. They were stored overnight at 6 °C in phosphate-buffered frog Ringer solution to which 5 mM-glucose and penicillin and streptomycin (100 mg l<sup>-1</sup>) were added. Almost all measurements were made in the cell-attached mode (Hamill *et al.* 1981). In one series of experiments the effect of varying the ionic composition of the intra- and extracellular solutions on end-plate channel gating behaviour was determined. The effect of intracellular ion composition on end-plate channel currents was measured on isolated inside-out patches of perijunctional membrane, which could occasionally be obtained in the following way. The preparation was washed in Ca<sup>2+</sup>-free frog Ringer solution for 10 min at 8–10 °C, to minimize contractions. Subsequently the bath was slowly perfused with Ca<sup>2+</sup>-free isotonic KCl (115 mM). About 20% of all fibres did not contract, or relaxed again without forming contraction clots. Isolated inside-out patches were obtained by air exposure of the pipette tip (Hamill *et al.* 1981), in a Ca<sup>2+</sup>-free bath solution which contained isotonic KCl and 0.5 mM-EGTA. In a few experiments these patches could be polarized to –150 mV.

### *Pipettes*

Most patch-clamp experiments were made with patch pipettes fabricated from soft glass (Cee-Bee). They had resistances of 2–5 MΩ when filled with frog Ringer solution and had the dimensions described by Sakmann & Neher (1983). A few experiments were made with hard glass (H5-10, Jencons Scientific) pipettes. Hard glass pipettes had resistances of 4–8 MΩ. All pipettes had a thick coat of Sylgard. No difference was noted in the channel conductance, or in the kinetics of channel opening and closing, between recordings made with pipettes fabricated from the two types of glass. Neither the glass type, nor the pipette resistance was obviously correlated with the success rate in obtaining gigohm seals.

### Filtering and recording

Records were filtered with an eight-pole Bessel-type filter (Barr & Stroud, in damped mode). Filter cut-off frequencies are given as the -3 dB frequency (half the value shown on the front panel for our filters).

During experiments the current and voltage signals were recorded on FM tape (Racal Store 4, Hythe). Usually signals were low-pass filtered at 10 kHz (eight-pole Bessel) before recording (to prevent saturation of the recorder by high-frequency noise), and recorded at 30 in. s<sup>-1</sup> (band width 10 kHz, -1 dB).

### Analysis

Signals from magnetic tape were filtered at 4–9 kHz (eight-pole Bessel) and the entire record was digitized continuously at up to 40 kHz (CED 502 interface, Cambridge Electronic Design, Cambridge). The sampling rate was 8–10 times the filter cut-off frequency (-3 dB). The positions of opening and shutting transitions were measured by fitting the time course of the signal, using the measured step response functions of the system (patch clamp, tape recorder and filters); the method was as described by Colquhoun & Sigworth (1983), with the addition of a facility to analyse contiguous open states so that conductance sublevels could be measured. The result was an idealized record of the duration and amplitude of every detectable event. This record was then revised to ensure a consistent time resolution throughout by imposition of a fixed minimum resolvable duration (Colquhoun & Sigworth, 1983, p. 224) which in a typical case, might be 40 µs for shut periods and 60 µs for openings. In the very best records 25 µs resolution for shut periods was considered to be safe.

Values for open times, shut times, burst lengths etc. were constructed from the revised record and used for (a) display of distributions as histograms and (b) fitting appropriate distributions by the method of maximum likelihood (Colquhoun & Sakmann, 1981; Colquhoun & Sigworth, 1983). Distributions were fitted, as appropriate, by the sum of several exponential terms or by the sum of several geometric terms (as in eqns. (4) and (11)). The results in Fig. 18 were fitted by a gamma distribution,  $\Gamma_k(t)$ . This is the distribution expected for the sum of  $k$  variables, when each variable has a simple exponential distribution  $\tau_0^{-1}e^{-t/\tau_0}$  with mean  $\tau_0$ . The distribution has mean  $k\tau_0$ , and is

$$\Gamma_k(t) = \frac{\tau_0^{-k} (t/\tau_0)^{k-1} e^{-t/\tau_0}}{(k-1)!}. \quad (1)$$

For  $k = 1$  this reduces to a simple exponential distribution (and for large  $k$  it tends toward a Gaussian distribution). The appropriate conditional distribution needed for fitting (see Colquhoun & Sigworth, 1983) when the data values are restricted to a range between, say,  $t_{\min}$  and  $t_{\max}$  is found by dividing this by  $P(t_{\min} < t < t_{\max}) = F(t_{\max}) - F(t_{\min})$  where the distribution function corresponding to  $\Gamma_k(t)$  is given by

$$F(t) = 1 - \sum_{r=0}^{k-1} \frac{(t/\tau_0)^r e^{-t/\tau_0}}{r!}. \quad (2)$$

### Definition of apparent openings, bursts and ‘long bursts’

Bursts of openings are defined as groups of openings that are separated by gaps that are all shorter than some specified length,  $t_c$ . In many cases the mean length of the gaps between bursts was several hundred-fold greater than the mean length of gaps within bursts so the choice of  $t_c$  was not critical. In a few cases, when the separation was less clear,  $t_c$  was chosen so as to make the proportion of long intervals that were misclassified (as short) equal to the proportion of short intervals that were misclassified (as long). This was achieved by solving for  $t_c$  the equation

$$1 - e^{-t_c/\tau_s} = e^{-t_c/\tau_m}, \quad (3)$$

where  $\tau_s$  and  $\tau_m$  are the slow and intermediate time constants in the distribution of all shut times (so ‘intermediate’ gaps as well as short gaps are classified as gaps within bursts). The criterion given in eqn. (3) differs from that of Jackson, Wong, Morris, Lecar & Christian (1983) who calculated  $t_c$  so as to minimize the total number of misclassifications; it also differs from that of Magleby & Pallotta (1983) and Clapham & Neher (1984), who calculated  $t_c$  so as to produce equal numbers of misclassifications for short and long intervals. When the numbers of short and long intervals differ considerably the last two methods (especially the former) may result in misclassification of a large

*proportion* of the rarer type of interval. However, the total number of misclassifications is smaller (and therefore the estimate of the number of bursts is more accurate) with the latter methods.

The results to be presented strongly suggest that there are many brief shut periods that are too short to be detected. Because of this the measured 'open times' will often be made up of more than one actual opening; they will therefore be referred to as '*apparent open times*'. There will also be some openings that are too short to be detected, although this problem is much less severe both because the openings are not so short and because brief openings are less numerous than brief gaps (except at very low agonist concentrations).

Values of open and shut times were fitted by the method of maximum likelihood with a probability density function that is the sum of one or more exponential terms, i.e.

$$f(t) = \sum_{i=1}^k a_i \lambda_i e^{-\lambda_i t}, \quad (4)$$

where  $a_i$  represents the area of the  $i$ th component ( $\Sigma a_i = 1$ ),  $\lambda_i = 1/\tau_i$  is its fitted rate constant, and  $\tau_i$  its time constant. The fitting process also provides an estimate of the number of events,  $N$ , including those outside the fitted range (Colquhoun & Sigworth, 1983, p. 246). Suppose, for example, that a burst length distribution is fitted by two exponentials with areas  $a_s$ ,  $a_f$  and time constants  $\tau_s$ ,  $\tau_f$  (where the subscripts stand for slow and fast respectively). It is, of course, incorrect in general to identify these components with particular physical events, or to refer to '*short bursts*' and '*long bursts*' as though these were separate sorts of phenomena. Nevertheless we shall use terms such as '*the number of short bursts*', defined as  $N a_f$ , for the following reasons: (1) the definitions are precise even if the words are not, (2) they constitute a convenient verbal shorthand, and (3) in some cases at least an approximate physical significance can be attached to the components (as, for example, in the case discussed by Colquhoun & Hawkes, 1982).

#### *Corrections for missed events*

The total open time in the record will be extended by the inadvertent inclusion of the time spent in undetected gaps. Suppose the distribution of all shut times is fitted by  $f_g(t)$  as in eqn. (4) above, and the estimated total number of shut times is  $N_g$ . The total time spent in gaps within bursts (i.e. by definition, gaps shorter than  $t_c$ ), including those that are undetected, can be estimated as

$$m_{TS} = N_g \int_0^{t_c} t f_g(t) dt = N_g \left[ m_g - \sum a_i (t_c + \tau_i) e^{-t_c/\tau_i} \right], \quad (5)$$

where  $m_g = \sum a_i \tau_i$  is the over-all mean gap length. If the fastest component has area  $a_{g,f}$  the '*number of short gaps*' is defined as  $N_{g,f} = N_g a_{g,f}$ . Suppose also that the burst length distribution is fitted with two exponentials with time constants  $\tau_{b,s}$ ,  $\tau_{b,f}$  and areas  $a_{b,s}$ ,  $a_{b,f}$ , the total number of bursts being  $N_b$ , the '*number of long bursts*' is then defined as  $N_{b,s} = N_b a_{b,s}$ , and the over-all mean burst length is  $m_b = a_{b,f} \tau_{b,f} + a_{b,s} \tau_{b,s}$ . The total time occupied by bursts is thus  $N_b m_b$  and the corrected total open time is  $m_{TO} = N_b m_b - m_{TS}$ , where  $m_{TS}$  is the total shut time within bursts (eqn. 5). Thus, for example, the corrected mean number of short gaps per unit open time can be estimated as  $N_{g,f}/m_{TO}$ , and the corrected mean number of short gaps per long burst is given by  $N_{g,f}/N_{b,s}$ . If we suppose (see Results) that '*short bursts*' contain few gaps then the total open time spent in long bursts is  $N_{b,s} \tau_{b,s} - m_{TS}$ , and the corrected mean length of an individual opening in a long burst is

$$(N_{b,s} \tau_{b,s} - m_{TS}) / (N_{g,f} + N_{b,s}). \quad (6)$$

#### *Tests of correlation between events*

Two sorts of tests were done to see whether, for example, the lengths of successive bursts were independent of one another, or whether a short burst tended to be followed by another short burst. These were the runs test (which is the more robust), and the calculation of autocorrelation coefficients.

The runs test (David & Barton, 1962) is calculated by converting a series of numbers (e.g. burst lengths) into a series consisting of the digits 0 and 1. For example a burst shorter than some critical time, e.g. 0.3 ms, might be counted as a 0, and a burst longer than 0.3 ms counted as 1. Say the series consists of  $n_0$  zero values and  $n_1$  unity values so the total number of observations is  $n_0 + n_1 = n$ . The number of runs,  $T$  say, in the series is then counted, a run being defined as a contiguous section

of the series that consists entirely of (one or more) 0 values, or entirely of 1 values (e.g. 110001 has three runs). If the series is in random order then the mean and variance of  $T$  will be

$$E(T) = \frac{2n_0 n_1}{n} + 1, \quad (7)$$

$$\text{var}(T) = \frac{2n_0 n_1 (2n_0 n_1 - n)}{n^2 (n-1)}. \quad (8)$$

The test statistic,  $z$ , defined as

$$z = [T - E(T)] / [\text{var}(T)]^{1/2}, \quad (9)$$

has an approximately Gaussian distribution with zero mean and unit standard deviation, so a value of  $|z|$  of greater than about 2 is unlikely to occur by chance. A positive correlation between the lengths of events will lead to there being fewer (though longer) runs than predicted by eqn. (7), so  $z$  will be negative.

The autocorrelation coefficient with lag  $m$ ,  $r_m$  say, is calculated from the original observations of, for example, burst length. If the observations are denoted  $y_i$  ( $i = 1, \dots, n$ ), with mean  $\bar{y}$ , then

$$r_m = \frac{\sum_{i=1}^{n-m} (y_i - \bar{y})(y_{i+m} - \bar{y})}{\sum_{i=1}^n (y_i - \bar{y})^2}. \quad (10)$$

If the observations are independent then this estimate will be approximately Gaussian with mean zero and variance  $1/n$ , so the test statistic  $r_m \sqrt{n}$  is appropriate. Autocorrelation coefficients were pooled by calculation of the weighted mean of their Fisher transformations.

## RESULTS

### *Shut states of the channel*

It is desirable to start by considering the lengths of time for which a channel stays shut ('gap lengths') because in so far as there are more shut states than open states the distribution of shut periods is more informative (and more complex) than that of open times (Colquhoun & Hawkes, 1982; Colquhoun & Sakmann, 1983), and because it is possible to define bursts of openings only after inspection of the gap distribution.

Fig. 1 shows records of single-channel currents evoked by ACh, SubCh and CCh. The brief interruptions of the channel openings are obvious. The distributions of the durations of all shut periods were fitted by a sum of exponentials as described in the Methods section. At low agonist concentrations three exponential terms were usually sufficient to describe the observations reasonably well, though at higher concentrations (at which desensitization and/or channel block became obvious) five or six exponentials were needed (as illustrated by Colquhoun & Sakmann, 1983). Fig. 2 shows an example of the distribution found with a low concentration (100 nm) of SubCh. The same simultaneous fit of three exponentials is shown (continuous line in Fig. 2) on three different time scales to display each of the time constants. The briefest gap component had a time constant of  $\tau_f = 45.4 \pm 2.0 \mu s$  and represented  $a_f = 75.0 \pm 1.3\%$  of the area under the distribution (Fig. 2C); the longest component had a time constant  $\tau_s = 274 \pm 14 \text{ ms}$ , and  $a_s = 21.2 \pm 1.2\%$  of the area (Fig. 2A). The intermediate component, with  $\tau_m = 1.3 \pm 0.2 \text{ ms}$ , had only  $a_m = 3.8 \pm 0.4\%$  of the area (or  $a_m \approx 4.8\%$  of the short gap area, slightly more than average (see Table 1). Despite

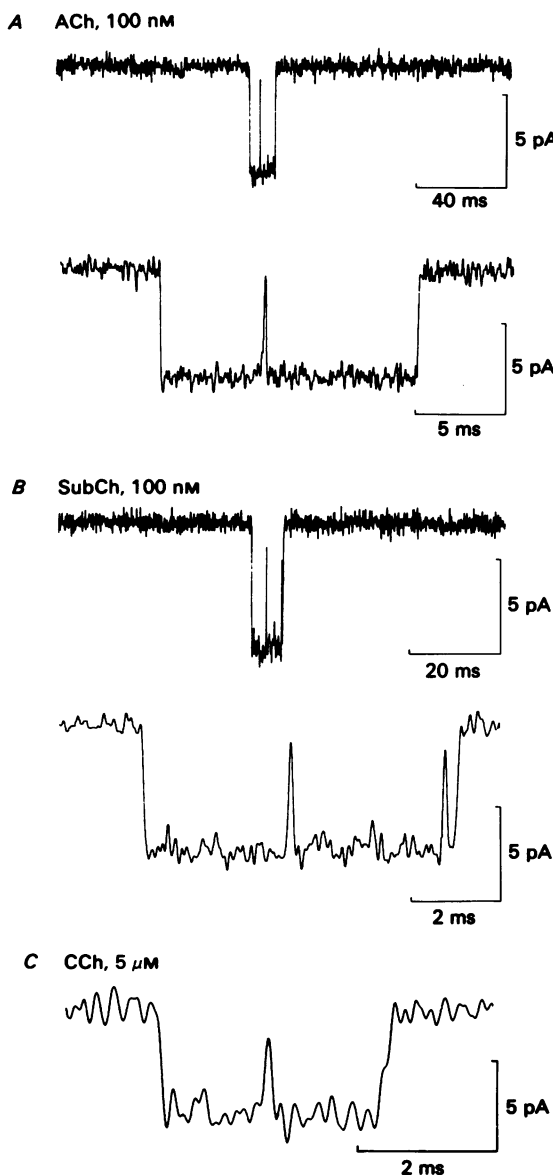


Fig. 1. Examples of elementary currents activated by three different agonists. *A*, single-channel current activated by 100 nM-ACh, shown at low- and high-time resolution. Membrane potential -182 mV, temperature 10.5 °C. The upper, low-time resolution trace shows that the elementary current is well separated in time from adjacent currents. The average frequency of occurrence of elementary currents in this recording was less than  $1\text{ s}^{-1}$ . At high-time resolution (lower trace) it is seen that this elementary current represents two resolved channel openings separated by a short closure. *B*, single-channel current activated by 100 nM-SubCh -175 mV, 11 °C. This elementary current consists of three resolved channel openings separated by two short channel closures. *C*, high resolution recording of an elementary current activated by 5  $\mu\text{M}$ -CCh, -160 mV, 12 °C. The elementary current is briefly interrupted once. All high-resolution traces were filtered at 4.5 kHz (-3 dB).

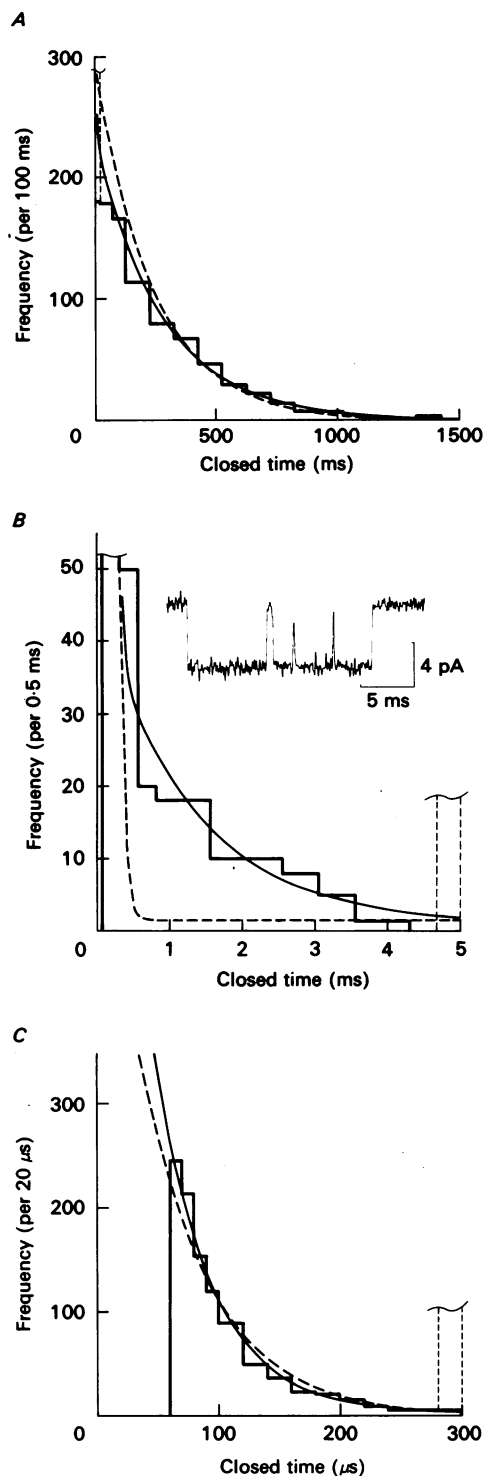


Fig. 2. For legend see opposite.

the smallness of this intermediate component it was detectable in almost every experiment and was reasonably reproducible (see Table 1). The dashed line (the best fit with two exponentials) shows the effect of its omission; the fit is obviously worse and is quite inadequate in the intermediate duration region (Fig. 2B). Furthermore the estimates of the fast and slow time constants are substantially altered if the intermediate component is omitted, the values that correspond to the dashed line in Fig. 2 being  $\tau_f = 56.4 \mu\text{s}$  ( $a_f = 72.5\%$ ) and  $\tau_s = 239 \text{ ms}$  ( $a_f = 27.5\%$ ).

The longest component presumably represents intervals between separate activations of ion channels so its duration is uninterpretable in the absence of information about the number of channels from which measurements are being made. But the two faster components are so brief that they must almost always represent interruptions of the opening caused by a single activation of one ion channel. The major fast component will be considered first; the mean duration of these gaps will be considered now, and their frequency will be described below after bursts have been defined.

#### *Short gaps during channel openings*

*Dependence of duration on the nature of the agonist.* The histograms in Fig. 3 illustrate the part of the distribution that shows the duration of the briefest gaps. It is obvious that the fast time constant,  $\tau_f$ , depends on the nature of the agonist, the briefest gaps being longest for DecCh ( $71 \mu\text{s}$ ) and shorter for SubCh ( $43 \mu\text{s}$ ), ACh ( $20 \mu\text{s}$ ) and CCh ( $13 \mu\text{s}$ ).

The average results for these agonists are shown in Table 1 and Fig. 4. These measurements, despite the brevity of the gaps, were among the most consistent made. For example in four separate sets of experiments with SubCh the values obtained were: September 1980,  $45.6 \pm 0.6 \mu\text{s}$  ( $n = 2$ ); June 1981,  $41.7 \pm 6.7 \mu\text{s}$  ( $4$ ); August 1982,  $43.5 \pm 2.2 \mu\text{s}$  ( $5$ ), and in February 1983,  $44.0 \pm 1.7 \mu\text{s}$  ( $4$ ).

It will be assumed later that the fitted distributions describe the data right down to zero duration; if this is so (and there is no direct evidence for this) the histograms in Fig. 3 show that there are many brief gaps that are too short to be seen. For example, with a resolution of  $40 \mu\text{s}$ , we should expect to see 56% of gaps with a mean

Fig. 2. Distribution of the durations of shut times in an experiment with  $100 \text{ nM}$ -SubCh at a membrane potential of  $-131 \text{ mV}$ . The record was filtered at  $2 \text{ kHz}$  ( $-3 \text{ dB}$ ), and the resolution set at  $70 \mu\text{s}$  for openings and  $60 \mu\text{s}$  for gaps. After imposition of the resolution there were 1337 gaps in the range used for fitting ( $60 \mu\text{s}$ - $1000 \text{ ms}$ ). The fit of three exponentials is shown as a continuous line, and the fit of two exponentials as a dashed line; the parameters of the fit are given in the text. The former fit implies that the record contains 3019.3 gaps altogether, 1665.5 being below  $60 \mu\text{s}$  and 16.8 above  $1000 \text{ ms}$ . A shows the whole distribution up to  $1500 \text{ ms}$ ; there were five observations above  $1500 \text{ ms}$  and the left-most bin, which represents many short gaps, is well off-scale (ordinate = 3128). B shows the same data and the same fitted curve up to  $5 \text{ ms}$ , to display clearly the intermediate component. Both bottom and top bins are off-scale (ordinates 631 and 1242 respectively). The inset shows a channel opening that contains three short gaps; the two on the right are very brief but the left-most gap is typical of those that appear in the intermediate component. C shows the same data and fitted curve up to  $300 \mu\text{s}$ ; the right-most bin is off-scale (ordinate = 731).

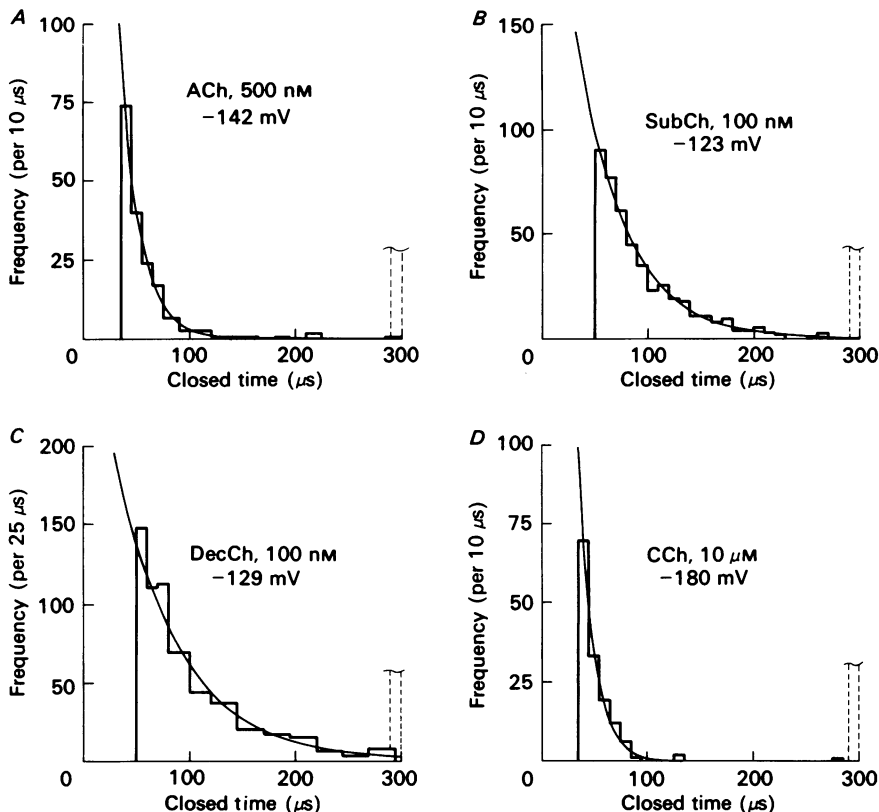


**Fig. 3.** The distribution of shut times for four agonists shown up to 300  $\mu$ s to emphasize the distribution of the shortest gaps. In each case the distribution has been fitted with at least three exponentials (as in Fig. 2). *A*, ACh, 500 nM. Membrane potential  $-142$  mV, temperature  $10.2$  °C. Resolution  $50\ \mu$ s for openings,  $35\ \mu$ s for gaps. The 575 gaps between  $35\ \mu$ s and  $10$  s were fitted with four exponentials; the time constants were  $18.1 \pm 1.3\ \mu$ s,  $0.39 \pm 0.15$  ms,  $138 \pm 23$  ms and  $1954 \pm 178$  ms, and the corresponding areas were,  $74.0 \pm 2.7\%$ ,  $1.5 \pm 0.4\%$ ,  $9.9 \pm 1.0\%$  and  $14.6 \pm 1.9\%$ , respectively. *B*, SubCh, 100 nM. Membrane potential  $-123$  mV, temperature  $12.5$  °C. Resolution  $70\ \mu$ s for openings,  $50\ \mu$ s for gaps. The 928 gaps between  $50\ \mu$ s and  $2$  s were fitted with three exponentials; the time constants were  $45.2 \pm 2.3\ \mu$ s,  $1.3 \pm 0.4$  ms and  $446 \pm 25$  ms, and the areas were  $74 \pm 1.4\%$ ,  $2.4 \pm 0.4\%$  and  $23.6 \pm 1.4\%$ . *C*, DecCh, 100 nM. Membrane potential  $-129$  mV, temperature  $9.8$  °C. Resolution  $60\ \mu$ s for openings,  $50\ \mu$ s for gaps. The 606 gaps between  $60\ \mu$ s and  $2.5$  s were fitted with three exponentials; the time constants were  $60.1\ \mu$ s,  $0.9$  ms and  $848$  ms, and the areas were  $69.6\%$ ,  $1.4\%$  and  $29.0\%$ . *D*, CCh, 10  $\mu$ M. Membrane potential  $-180$  mV, temperature  $10.5$  °C. Resolution  $60\ \mu$ s for openings,  $35\ \mu$ s for gaps. The 949 gaps between  $35\ \mu$ s and  $500$  ms were fitted with three exponentials; the time constants were  $14.1\ \mu$ s,  $2.2$  ms and  $108$  ms, and the areas were  $67.7\%$ ,  $0.5\%$  and  $31.8\%$ .

lifetime of  $70\ \mu$ s,  $37\%$  of gaps with a mean lifetime of  $40\ \mu$ s, and  $13.5\%$  of gaps with a mean lifetime of  $20\ \mu$ s.

*Dependence of duration on agonist concentration.* The time constant for the brief gap component appeared to be independent of agonist concentration over the range tested with SubCh, ACh and CCh. This is shown in Fig. 4. The most complete results are

for SubCh which showed no detectable change in  $\tau_f$  over a 625-fold range of concentration, from 4 to 2500 nM.

*Dependence of duration on membrane potential.* Although the majority of experiments were done at membrane potentials between -120 mV and -140 mV, some were done at other potentials, from -80 to -270 mV. The results are shown in Fig. 5. The time constant of the short gaps,  $\tau_f$ , shows no significant dependence on membrane

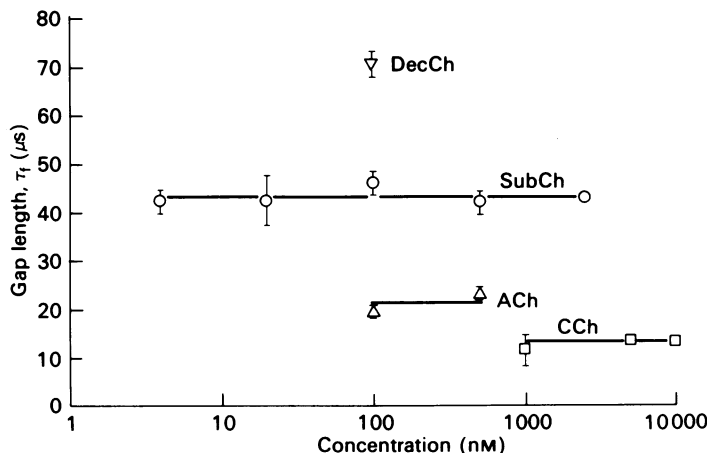


Fig. 4. Dependence of the time constant for the briefest gap component on agonist concentration.  $\nabla$ , DecCh;  $\circ$ , SubCh;  $\triangle$ , ACh;  $\square$ , CCh. No concentration dependence was detectable for SubCh, ACh or CCh.

potential, with the possible exception of SubCh which shows, if anything, a tendency to get shorter on hyperpolarization; the slope of the least-squares line for SubCh shown in Fig. 5 has a slope of  $2.9 \pm 1.3 \text{ V}^{-1}$  ( $P \approx 0.05$ ) which suggests that a change of membrane potential of 343 mV (95 % confidence limits 175–8152 mV) is needed for an e-fold change in  $\tau_f$ .

*Non-exponential distributions below 300  $\mu\text{s}$ .* In most cases the distributions of gap length from 30–50  $\mu\text{s}$  up to 300  $\mu\text{s}$  were fitted rather well by a single exponential component, as illustrated in Fig. 3. However, in some cases there were clear signs of still briefer gaps. This was particularly apparent in the experiments with the highest resolution, at hyperpolarized membrane potentials (which allow high resolution), and with agonists such as DecCh for which  $\tau_f$  is relatively long. The most obvious example is shown in Fig. 6. The resolution for gaps was set at 45  $\mu\text{s}$  in this experiment. As shown in Fig. 6, the usual three-exponential fit does not describe the data well in the region between 45 and 65  $\mu\text{s}$ , but an extra superfast exponential is required. This superfast component was clearly visible in only a few experiments (and not sufficiently well defined to be accurately estimated in any). However, a substantial number of experiments showed slight deviations of the fitted line in the 30–300  $\mu\text{s}$  region which suggested that the phenomenon could be quite general.

### The intermediate gap component

It has been consistently observed that the fitting of the distribution of shut periods can be improved if an intermediate component with a time constant of the order of 1 ms is included. This was illustrated in Fig. 2 in which the omission of this component was seen to produce an obviously poor fit. The results are summarized in Table 1. The scatter of the values for the intermediate component is considerably greater than

TABLE 1. Shut time distribution

Agonist	$\tau_f(\mu\text{s})$	$a'_f(\%)$	$\tau_m(\text{ms})$	$a'_m(\%)$
ACh	$20.2 \pm 1.0$ (8)	$96.6 \pm 0.7$ (8)	$0.51 \pm 0.18$ (8)	$3.4 \pm 0.7$ (8)
SubCh	$43.0 \pm 1.6$ (16)	$97.1 \pm 0.4$ (11)	$1.2 \pm 0.2$ (11)	$2.9 \pm 0.4$ (11)
DecCh	$70.6 \pm 2.6$ (5)	$97.7 \pm 0.8$ (5)	$0.66 \pm 0.14$ (5)	$2.3 \pm 0.8$ (5)
CCh	$13.2 \pm 0.8$ (10)	$98.2 \pm 0.5$ (7)	$0.13 \pm 0.03$ (7)	$1.8 \pm 0.5$ (7)

Measurements of the time constants for the short ( $\tau_f$ ) and intermediate ( $\tau_m$ ) gap lengths, and the relative areas  $a'_f = a_f/(a_f + a_m)$ , and  $a'_m = a_m/(a_f + a_m)$  that correspond to these two components in the distribution of all shut times. Measurements were made at membrane potentials from  $-120$  to  $-140$  mV, and several agonist concentrations. SubCh concentrations of 500 nM or more, and CCh at 1  $\mu\text{M}$ , have been omitted from the average values for the intermediate component. The number of values averaged is shown in parentheses.

that for the short-gap component, as might be expected given the smallness of this component. For example the mean time constant,  $\tau_m$ , of 1.2 ms for SubCh, has a standard deviation of 0.7 ms; nevertheless the results are quite sufficiently consistent to verify the genuineness of the intermediate component. The time constant appears to be shorter for ACh (0.5 ms), and for CCh (0.13 ms) than for SubCh (1.2 ms), but any difference between agonists in the area (relative to the shortest gaps) of the intermediate components was too small to be detected; it represented 2–3 % of the area for all agonists (see Table 1).

No consistent effect of membrane potential was observed (e.g. for SubCh the plot of  $\log(\tau_m)$  against membrane potential had a slope of  $-7.3 \pm 8.6 \text{ V}^{-1}$ ).

There was also no very consistent effect of SubCh concentration on the time constant of the intermediate component, but there was a suggestion that the area of this component increased with agonist concentration. The two most reliable experiments with 4 nM-SubCh gave a relative area ( $a'_m$ , see Table 1) of 1.1 % and 1.3 %. The corresponding values for 20 nM and 100 nM were undistinguishable ( $3.0 \pm 0.4$  % and  $2.7 \pm 0.5$  % respectively), but with 500 nM-SubCh three experiments gave 9.7 %, 8.7 % and 6.1 % (though a fourth experiment at  $-197$  mV did not allow clear identification of the intermediate component). The values for 500 nM-SubCh have been omitted from the mean given for SubCh in Table 1.

### Subconductance states

Many channel closures were so brief that the observed signal did not reach the base-line level (see Figs. 2 and 11). In order to take advantage of the increased time resolution provided by ‘time course fitting’ of such incompletely resolved events one must assume some value for the amplitude of the underlying events, because the

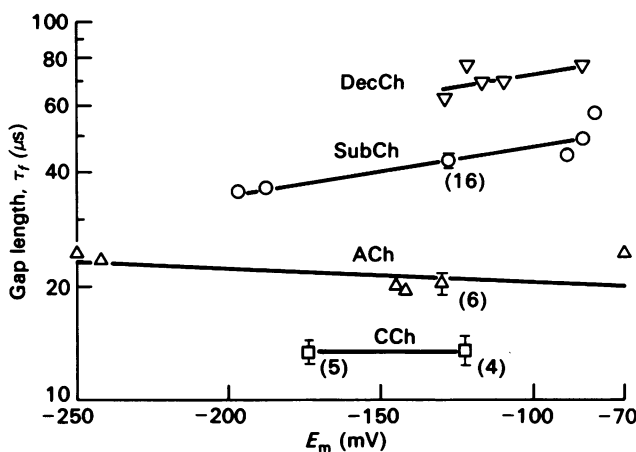


Fig. 5. Dependence of the time constant for the briefest gap component on membrane potential.  $\nabla$ , DecCh;  $\circ$ , SubCh;  $\triangle$ , ACh;  $\square$ , CCh. Values for similar potentials have been averaged (points with s.e. bars, marked with number of experiments in parentheses), and plotted against the mean potential to clarify the presentation; other points represent single experiments. In no case does the slope of the line differ significantly from zero with the possible exception of SubCh ( $P \approx 0.05$ ).

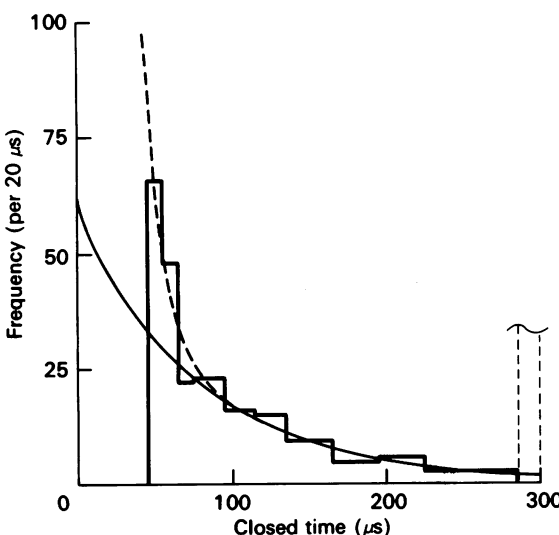
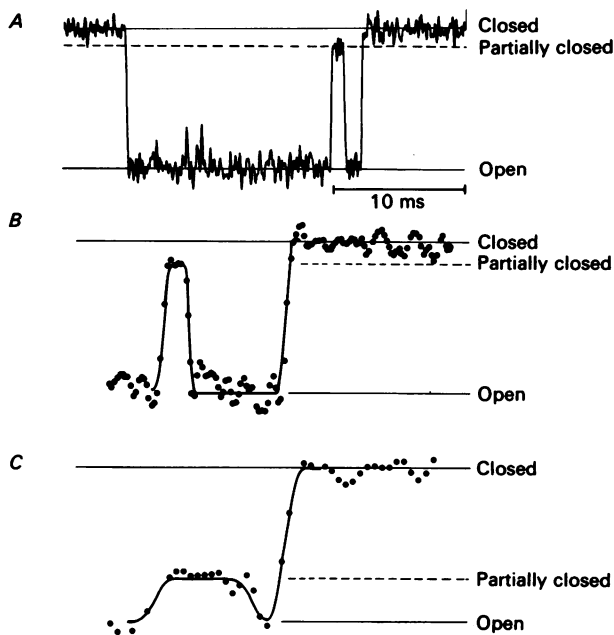


Fig. 6. An extreme example of deviation from a simple exponential distribution of shut times below 300  $\mu$ s. Agonist was DecCh, 100 nM, membrane potential -208 mV, temperature 9.8 °C. The continuous line shows a conventional three-exponential fit (from 70  $\mu$ s to 2 s); the time constants (with areas in parentheses) were 80  $\mu$ s (67.9%), 0.65 ms (4.7%), 980 ms (27.4%). The dashed line shows a four-exponential fit (from 45  $\mu$ s to 2 s); the parameters were 11.1  $\mu$ s (84.8%), 83.1  $\mu$ s (10.2%), 0.68 ms (0.7%), 977 ms (4.3%).

amplitude cannot be precisely estimated from the data (see Colquhoun & Sigworth, 1983). We have assumed that the brief interruptions represent complete closures of the channel, except on those rare occasions on which this assumption provided an obviously poor fit (see Fig. 8). It has been found, however, that ACh-activated channels in cultured muscle cells can adopt states ('subconductance states') in which



**Fig. 7.** Examples of single-channel current sublevels. *A*, elementary current activated by 100 nM-ACh.  $-125$  mV,  $11$  °C. The two continuous horizontal lines, marked closed and open respectively, represent the patch current when a channel is either completely closed or completely open. The average amplitude of the current through the fully open channel is  $-3.71$  pA. The dashed horizontal line represents the amplitude of a current sublevel. During the sublevel the channel is partially closed. The sublevel amplitude is  $-0.52$  pA, i.e. 14% of the full amplitude. *B* and *C*, partial channel closures in another patch with 500 nM-ACh at  $-178$  mV and  $10$  °C. The time course of the digitized current record (●) is fitted (continuous line) by the same step response function as was used for full openings and closings. However, it was assumed that the amplitudes of the current sublevels (marked partially closed) are 17% and 72%, respectively, of the full current amplitude. Sublevel amplitudes are indicated by the horizontal dashed line. The current through the fully open channel is  $-5.6$  pA in (*B*) and  $-5.7$  pA in *C*. The duration of the partial closures is  $310\ \mu s$  and  $360\ \mu s$  in *B* and *C* respectively. Filtered at 4 kHz ( $-3$  dB).

the channel is only partially closed. This was inferred from the observation that the current through an open channel shows direct transitions between a main amplitude level where the channel is fully open and a less frequently occurring lower level of amplitude (Hamill & Sakmann, 1981; Auerbach & Sachs, 1983; Takeda & Trautmann, 1984). Such partial closures also occur occasionally in the end-plate channel of frog muscle, as illustrated by the currents shown in Fig. 7. About 0.4% of all gaps within

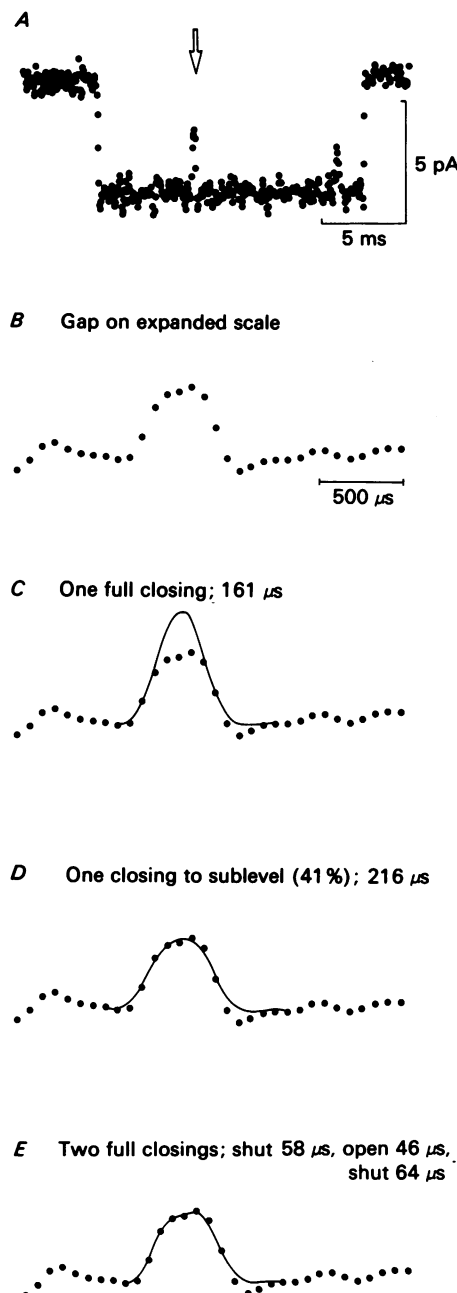
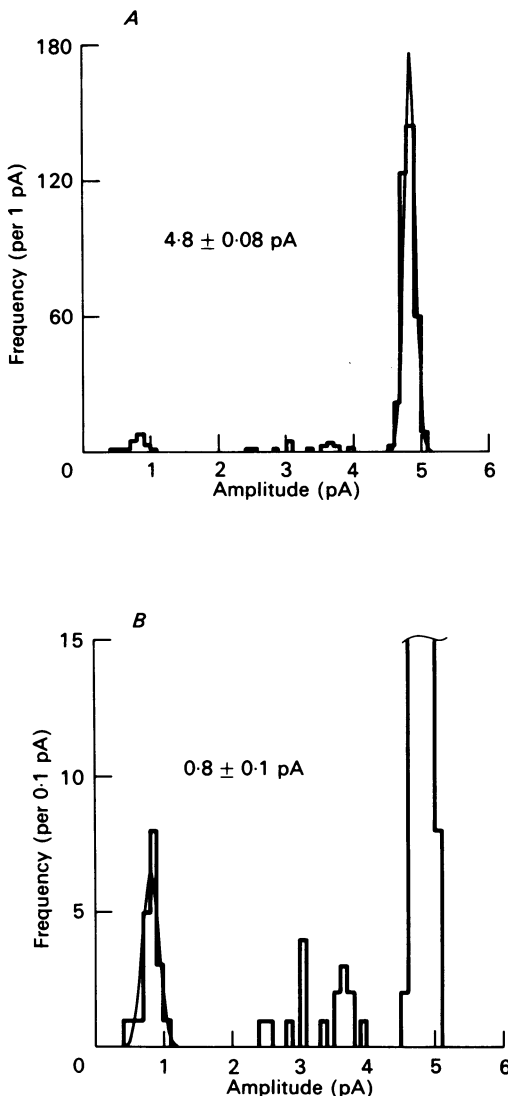


Fig. 8. Illustration of the problem of distinguishing subconductance states from multiple transitions. *A*, burst induced by SubCh, 100 nM, at  $-128$  mV. Two putative brief gaps are visible. Low-pass filter at 3 kHz ( $-3$  dB). *B*, the gap that is marked with an arrow in *A* shown on an expanded time scale. *C*, fit of data in *B* assuming a single complete closure of duration 161  $\mu$ s. *D*, fit of data in *B* assuming a single closure to a subconductance state, of duration 216  $\mu$ s. *E*, fit of data in *B* assuming that a full closure of 58  $\mu$ s is followed by a full opening of 46  $\mu$ s, and then another full closure of 64  $\mu$ s.



**Fig. 9.** Distribution of main and sublevel amplitudes in a single experiment. 100 nM-SubCh,  $-160$  mV,  $11$  °C. The main peak of the histogram shows the amplitudes of 355 openings. 36 of these ( $\approx 10\%$ ) show transitions to lower current levels which were fitted assuming them to be subconductance states. No minimum duration for the substate was imposed for the fit. *A*, low-resolution histogram. This illustrates the low proportion of sublevels in comparison with the main level. Mean of the main level is  $-4.8 \pm 0.08$  pA; it is fitted with a single Gaussian distribution. *B*, high-resolution histogram. This illustrates the scatter of the sublevel amplitudes. One well defined peak in sublevel amplitudes is found at  $-0.8$  pA. This corresponds to 17% of the main level amplitude. This peak of sublevel amplitudes represents partial closures such as those illustrated in Fig. 7*B*. These sublevel amplitudes are fitted by a single Gaussian distribution. Note the scattered distribution of other sublevel amplitudes between  $-2.5$  and  $-4$  pA.

bursts were unambiguous partial closures; 1–2 % of all long bursts contained a partial closure.

The current shown in Fig. 7A initially switches from the zero-current (shut) level to the main (fully open) level of 4.02 pA. Thereafter the current switches back transiently to a sublevel of 0.65 pA amplitude, i.e. there is a brief partial closure of the channel. Subsequently the channel reopens and then closes completely. In Fig. 7B and C the trace has been digitized and is fitted by the superposition of a full opening followed by a partial closing using the method of time course fitting. The subconductance state in Fig. 7C has a much larger amplitude than that shown in Fig. 7B. In the examples shown in Fig. 7 the duration of the partial closures is sufficiently long to obtain an unequivocal estimate of the amplitude of the sublevel.

#### *Ambiguity in detection of subconductance states*

Occasionally a gap was encountered which, although brief as judged by the fact that the current did not reach the base-line level, was nevertheless clearly not fitted well on the assumption that it represented a single full closure. An example is shown in Fig. 8. The SubCh-induced burst in Fig. 8A appears to contain two brief closures. The first of these, which is marked with an arrow in Fig. 8A, is shown on an expanded time scale in Fig. 8B. The fit based on the assumption that it represents a single complete closure is shown in Fig. 8C; it is obviously unsatisfactory. The time course can, however, be fitted almost equally well by either a single brief (216  $\mu$ s) closure to a subconductance level (of about 41 % of the full amplitude) as shown in Fig. 8D, or by two full closures separated by a short full opening, in quick succession, as in Fig. 8E. Events of the sort shown in Fig. 8 were rare, though in one experiment with SubCh (100 nm) as many as 15 were seen out of 505 openings. In such cases it is clear from Fig. 8D and 8E that it is impossible to be sure whether or not a subconductance state has occurred, and equally it is impossible to be sure whether or not a brief opening (46  $\mu$ s in Fig. 8E) has occurred in the middle of a burst (which is unfortunate because of knowledge of transitions within a burst between the two putative open states would be informative about mechanisms; see Discussion).

Fig. 9 shows the distribution of amplitudes of single-channel currents in an experiment with SubCh (100 nm at  $-161$  mV) in which every ambiguous gap of the type shown in Fig. 8 was fitted as though the closure were to a subconductance state. The main peak (Fig. 9A) has an amplitude of  $4.8 \pm 0.08$  pA. There are some lower amplitudes too, which are shown more closely on an expanded scale in Fig. 9B. Some of them are scattered between 2 and 4 pA (which suggests that these may have been double closures rather than genuine subconductance states), but there is a clear peak of low conductance states which has been fitted with a Gaussian curve ( $0.80 \pm 0.12$  pA) in Fig. 9B. This indicates the occurrence of a genuine subconductance state with an amplitude of about 17 % of main peak (though the standard deviation of this peak is 50 % greater than that of the main peak).

#### *Subconductance amplitude and duration*

The result in Fig. 9 suggests that discrete subconductance levels can be detected. Clearly a closure must be fairly long if we are to be sure that it represents closure to a subconductance level; with our most common filter setting of 3 kHz ( $-3$  dB)

a closure will reach 99.5% of its eventual amplitude in 250  $\mu\text{s}$ , and 97.6% in 200  $\mu\text{s}$  (Gaussian filter approximation: Colquhoun & Sigworth, 1983). We have therefore analysed, in a series of experiments, all subconductance states (those that could not be fitted adequately by a single full closure) that (a) were longer than 250  $\mu\text{s}$  and (b)

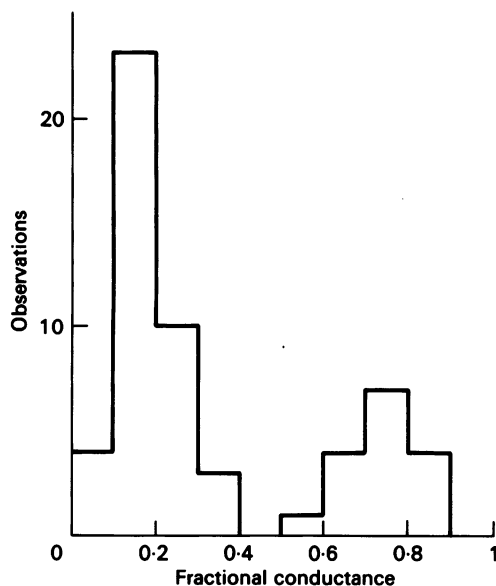
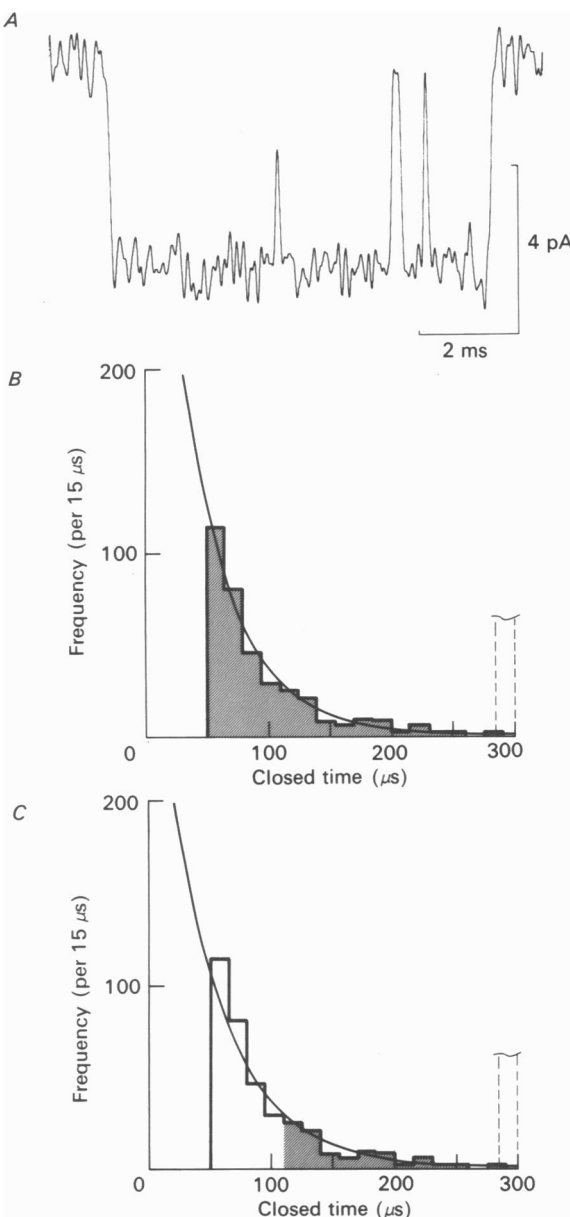


Fig. 10. Distribution of fully resolved current sublevels. The pooled data from sixteen different patches, with various agonists, 9.5–12 °C, -140 mV and -190 mV. In each individual recording from one patch the amplitude of the observed sublevels was normalized with respect to the amplitude of the main current level. Only sublevels occurring as a transient current decrease from the main level to a sublevel followed by a transition back to the main level (see Fig. 7, for examples) were included. All sublevels had durations of at least 250  $\mu\text{s}$ . The means of the two peaks in this distribution correspond to conductance substates of 18% and 71% of the main conductance state. The relative areas of the two peaks are 70% and 30% respectively.

were flanked on each side by a sojourn at the fully open level (as illustrated in Fig. 7). These criteria for distinguishing genuine subconductances are somewhat subjective, but the number of subconductances is small so we have adopted this method to allow some estimate to be made of their nature. The amplitude of such subconductance states was expressed as a fraction of the full amplitude. Fig. 10 shows the distribution of such fractional substate conductances observed in records from sixteen patches with various agonists (3023 long bursts were measured altogether). Clear peaks are visible at about 18% and 71% of the main conductance.

The total number of subconductances observed was too small to allow an accurate estimate of their duration. In the six best experiments (with three to eight clearly resolved sublevels in each) the mean duration (after subtraction of the resolution, 0.25 ms) was  $0.3 \pm 0.1$  ms (s.e. of mean). On this basis the number of unresolved sublevels would be of the same order as the number that were resolved, so the total number would still be small.



**Fig. 11.** Illustration of fit of all resolvable gaps in comparison with fit of only those gaps that reach the base line. SubCh, 100 nM, at  $-161$  mV. Filtered at  $4.5$  kHz. The resolution was set conservatively to  $50\ \mu s$  for gaps and  $70\ \mu s$  for openings so the first gap in the burst illustrated in *A*, which has a duration of about  $50\ \mu s$ , is the shortest that would be included. (Analysis with a resolution of  $40\ \mu s$  for gaps gives a similar result.) *B*, all shut times (shown only up to  $300\ \mu s$  in the histogram) from  $50\ \mu s$  to  $1400\ \mu s$  were fitted by the sum of three exponentials (continuous line). The time constants (and percentage areas) were  $39.8\ \mu s$  ( $70.2\%$ ),  $0.52\ ms$  ( $4.6\%$ ) and  $339\ ms$  ( $25.2\%$ ). *C*, the same data are fitted but all intervals shorter than  $110\ \mu s$  were excluded. The three-exponential fit (continuous line) was performed with the time constant and area of the intermediate component constrained to the values found above ( $0.52\ ms$ ,  $4.6\%$ ). The fast component had a time constant of  $45.5\ \mu s$  ( $65.8\%$ ) and the slow component was  $339\ ms$  ( $29.6\%$ ).

*Do brief gaps represent complete closures?*

It is clearly important to know whether brief gaps represent complete closures, if we are to be able to interpret the brief gaps in terms of the channel mechanism. Even if only a proportion, rather than all of the brief gaps represented closures to a subconductance state our estimates of the frequency and duration of brief closures could be seriously affected. The fact that the most common subconductance has an amplitude of only 18 % of the full level makes distinction between this and a full closure particularly difficult. The only way to determine unambiguously the properties of complete closures is to take into account only those gaps that clearly reach the base line. At our best resolution (filter set at 4.5 kHz, -3 dB) a closure of 110  $\mu$ s would attain 94 % of its eventual level, i.e. it would reach within 6 % of the base line if it were a complete closure. Therefore we have analysed the shut times in an experiment with SubCh (100 nm, -161 mV filtered at 4.5 kHz) both in the normal way, taking into account all resolvable gaps (assumed to be full closures), and by rejecting all gaps shorter than 110  $\mu$ s. Fig. 11A shows a burst with three interruptions. The last two of these reach the base line and so would be included in both analyses, but the first goes only about 58 % of the way down (duration about 50  $\mu$ s) and so would be included only in the former analysis.

The distribution of gap lengths is shown, up to 300  $\mu$ s, in Fig. 11B and C. The data are the same in both, but in Fig. 11B gaps from 50  $\mu$ s upwards have been fitted whereas in Fig. 11C only gaps longer than 110  $\mu$ s have been fitted. The usual three-component fit to all gap durations gave a time constant for the shorter component of 40  $\mu$ s in Fig. 11B and 46  $\mu$ s in Fig. 11C. The latter value is only marginally different from the fit that takes into account all closures longer than 50  $\mu$ s, most of which do not reach the base line. The value of 46  $\mu$ s is also close to the mean of all experiments with SubCh. The similarity of the two estimates of the duration of interruptions suggests that the possible inclusion of unresolved partial closures does not greatly affect our estimates of the duration of complete closures.

*Conclusions concerning subconductance states*

With all agonists more than 90 % of all short interruptions of the single-channel current do not reach the base line completely. For the remainder of this article we will, however, make the assumption that the majority of these interruptions represent complete channel closures. The main arguments for making this assumption are (a) the infrequent occurrence of resolved partial closures (relative to the number of resolved complete closures), (b) the similarity of short-gap characteristics when they are estimated from either resolved complete closures only or from all detectable gaps, and (c) the fact that most incompletely resolved 'partial closures' can equally well be fitted by the adjacent occurrence of two complete closures.

*Open states of the channel*

It was pointed out above that the form of the distribution of shut times suggest that there are many brief shut periods that are too short to be observed. If this is the case, then an individual single-channel 'opening' within a burst actually itself consists of a partially resolved burst of openings (A. G. Hawkes & D. Colquhoun, in

preparation), and the mean length of this 'apparent opening' (see Methods) will depend on the resolution of the data and on the brevity of the gaps. For this reason Colquhoun & Sakmann (1981, 1983) suggested that open-time distributions have no simple significance, though they can be interpreted by the more elaborate methods of A. G. Hawkes & D. Colquhoun (in preparation). In order to circumvent this problem it was suggested that a *burst* of openings should be defined as a series of openings which are separated by gaps which are all shorter than some specified length,  $t_c$ . In a typical case the gap distribution may be described by three exponentials with time constants of say 45  $\mu$ s, 1 ms and 800 ms. Therefore if  $t_c$  is chosen as, say, 5 ms, the first two classes of gap will almost all be counted in 'gaps within bursts' while the last class will almost all be counted in 'gaps between bursts' (eqn. (3) gives  $t_c = 5.1$  ms with 0.6% misclassification). Clearly the length of a burst, unlike that of an individual apparent opening, will be little affected by failure to detect short gaps, so this is an appropriate variable to work with (indeed before the present level of resolution was attainable a burst, as defined here, is what was called an opening because hardly any of the gaps within the burst were detectable). Typical bursts of openings are illustrated in Figs. 1 and 12. When channel activations are infrequent the choice of  $t_c$  is not critical and the division of the record into bursts is unambiguous (see Methods). When activations are frequent (e.g. at higher agonist concentrations) the process becomes more unreliable (especially when the intermediate gaps are included as gaps within bursts, as was our usual practice).

#### *The distribution of the burst length*

It was usually found that two exponentials were needed to fit the distribution of the burst length, and also to fit the distribution of the total open time per burst (which is very similar to the burst length since the total shut time within a burst is small). The latter observation suggests that there are at least two sorts of open state (Colquhoun & Hawkes, 1982). Under most conditions the slower component (time constant  $\tau_s$ , area  $a_s$ ) is predominant, but in low agonist concentrations the fast component ( $\tau_f$ ,  $a_f$ ) becomes more obvious (see below). Typical records obtained with ACh, SubCh, DecCh and CCh are shown in Fig. 12. The distributions observed with four agonists are illustrated in Fig. 13, and the results summarized in Table 2.

*The slower component.* The predominant (slower) component is longest for SubCh and DecCh, shorter for ACh and shortest for CCh. This order, and absolute values of  $\tau_s$ , are in good agreement with values of the so-called 'mean open-channel lifetime' inferred from noise analysis.

As expected from many earlier studies,  $\tau_s$  gets longer with hyperpolarization. From a linear fit to  $\log(\tau_s)$  against  $E_m$  we find for SubCh,  $\tau_s = 3.6 \pm 0.3$  ms at -90 mV or  $7.5 \pm 0.4$  ms at -130 mV; a hyperpolarization of  $55 \pm 6$  mV produces e-fold lengthening. For ACh,  $\tau_s = 2.0 \pm 0.6$  ms at -90 mV and  $4.2 \pm 0.4$  ms at -130 mV, with  $54 \pm 20$  mV for an e-fold lengthening. For CCh,  $\tau_s = 0.78 \pm 0.15$  ms at -90 mV and  $1.3 \pm 0.1$  ms at -130 mV, with  $82 \pm 23$  mV for an e-fold lengthening. It is doubtful whether the voltage dependence is significantly different for different agonists.

There was no clear dependence of the predominant burst length,  $\tau_s$ , on agonist concentration over the range tested for ACh, SubCh or CCh. At a membrane potential of -120 to -140 mV we found the following. For SubCh at 4 nM,  $\tau_s = 8.2 \pm 1.3$  ms

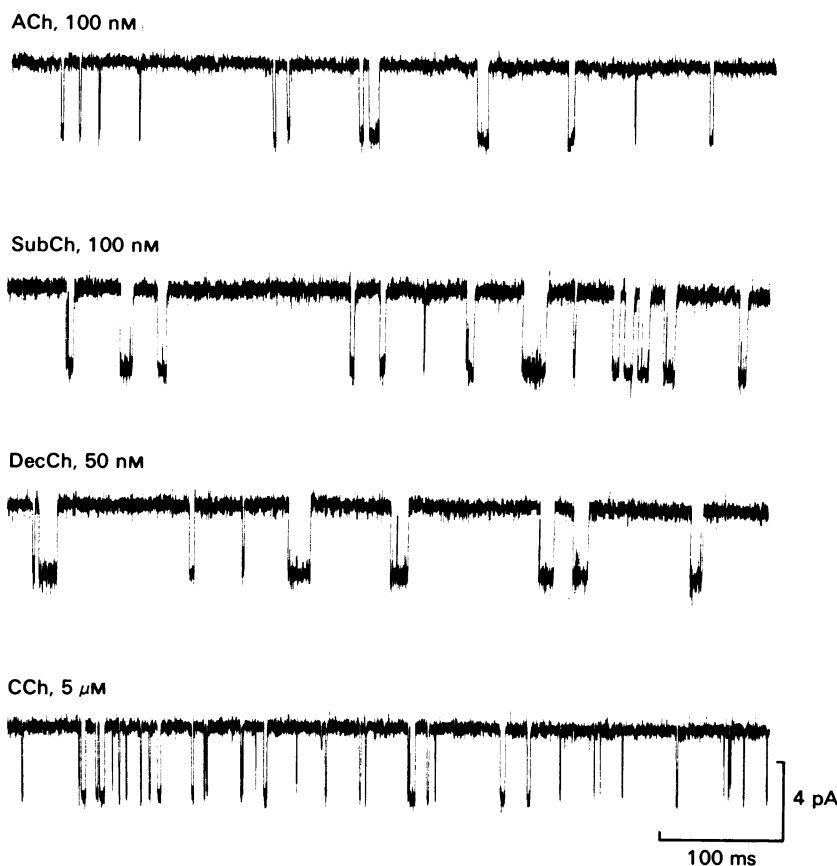


Fig. 12. Elementary currents activated by ACh and its analogues at the end-plate. These records illustrate the differences in average duration of elementary bursts. Four different patches in different fibres. ACh, 100 nM, -130 mV, 10 °C: mean duration of long bursts was 4.2 ms. SubCh, 100 nM, -130 mV, 12 °C: mean burst duration was 7.4 ms. DecCh, 50 nM, -120 mV, 11 °C: mean burst duration was 12 ms. CCh, 5  $\mu$ M, -130 mV, 9 °C: mean burst duration was 1.8 ms. All records filtered at 2 kHz (-3 dB).

( $n = 3$ ); at 20 nM,  $\tau_s = 7.4 \pm 1.1(4)$ ; at 100 nM,  $\tau_s = 7.2 \pm 1.0(5)$  and at 500 nM,  $\tau_s = 9.7 \pm 0.7(3)$ . Similarly for ACh at 100 nM,  $\tau_s = 4.2 \pm 0.4$  ms, and at 500 nM,  $\tau_s = 4.2 \pm 0.6$  ms.

*The faster component.* The time constant of this component was estimated with relatively low precision in many experiments in which the number of short bursts was relatively small. Within experimental error it was not possible to detect any effect of agonist concentration or membrane potential on  $\tau_f$  so all values have been pooled in Table 2. It was, however, clear that 'short bursts' were much more common at low agonist concentrations. Fig. 17 (see below) shows the distribution of the open time per burst for three concentrations of SubCh (this distribution is very similar to that of the burst length because of the brevity of the shut periods within a burst, but is somewhat simpler theoretically). The number falling in the shortest time bins is clearly greatest with the lowest concentration. The areas,  $a_s$  and  $a_f$ , for the two components are illustrated by the shaded areas in Fig. 14A and B and their ratio,

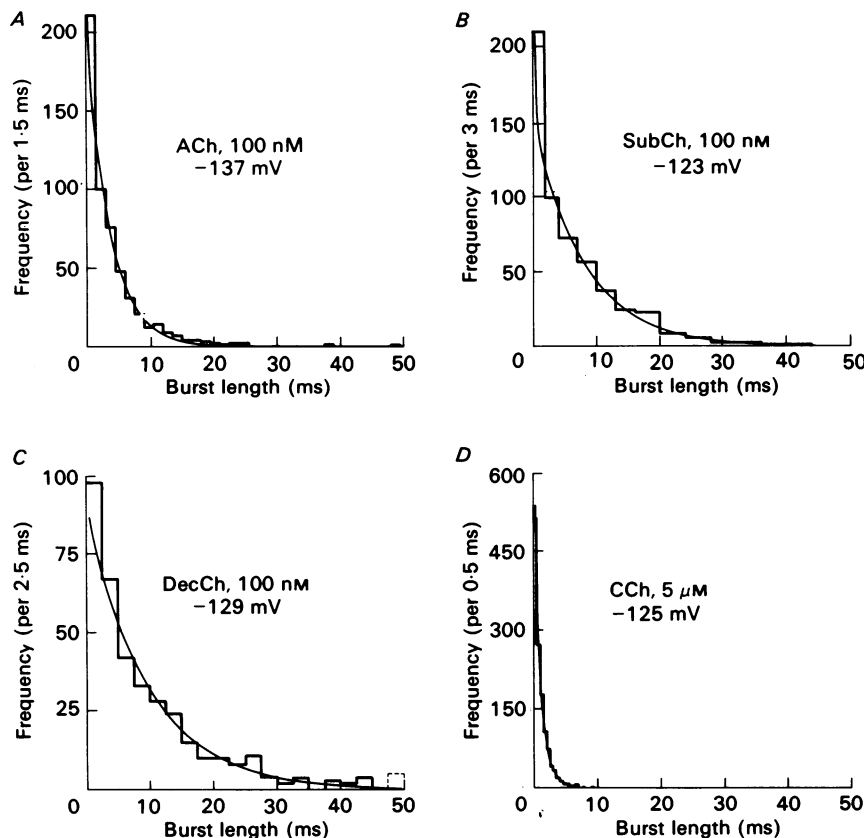


Fig. 13. Distribution of the burst length for ACh and three other agonists. The distributions are fitted with two exponentials (continuous line) and are plotted up to 50 ms for each agonist to facilitate comparison between them. *A*, ACh, 100 nM. Membrane potential  $-137$  mV. Resolution  $50\ \mu\text{s}$  for openings,  $35\ \mu\text{s}$  for gaps. Critical gap length for definition of bursts  $0.5$  ms. The time constants were  $0.12$  and  $3.7$  ms, and the areas were  $11\%$  and  $89\%$  respectively. *B*, SubCh, 100 nM. Membrane potential  $-123$  mV. Resolution  $70\ \mu\text{s}$  for openings,  $60\ \mu\text{s}$  for gaps. Critical gap length  $3$  ms. The time constants were  $0.16$  and  $8.0$  ms and the areas were  $15\%$  and  $85\%$  respectively. *C*, DecCh, 100 nM. Membrane potential  $-129$  mV. Resolution  $60\ \mu\text{s}$  for openings,  $50\ \mu\text{s}$  for gaps. Critical gap length  $3$  ms. The time constants were  $0.07$  and  $9.3$  ms and the areas were  $14\%$  and  $86\%$  respectively. *D*, CCh,  $5\ \mu\text{M}$ . Membrane potential  $-125$  mV. Resolution  $60\ \mu\text{s}$  for openings,  $35\ \mu\text{s}$  for gaps. Critical gap length  $0.5$  ms. The time constants were  $0.20$  and  $1.16$  ms and the areas were  $13\%$  and  $87\%$  respectively.

$a_s/a_t$ , is plotted against SubCh concentration (with double logarithmic coordinates) in Fig. 14*C*. The relative number of short openings clearly increases rapidly as the concentration is reduced below  $20\text{ nM}$ . The graph has an initial slope close to unity (indicated by the dashed line in Fig. 14*C*), though the slope becomes much shallower at higher concentrations. When plotted on arithmetic coordinates the initial slope is about  $1.7 \times 10^8\text{ M}^{-1}$ , a value that may give useful information about mechanisms (see Discussion).

The same tendency was seen for ACh also; the proportion of the total area of the

burst length distribution accounted for by the brief component was  $24 \pm 5\%$  at 100 nm-ACh and  $9.5 \pm 4\%$  at 500 nm-ACh.

*Very long bursts.* In most runs a small number of bursts were seen that were too long to be fitted by the distributions described above. This happened sufficiently often for there to be little doubt that it was a real phenomenon. Such extra-long bursts usually contained many short gaps but they were too rare for any detailed analysis to be done on them.

TABLE 2. Burst length distribution

Agonist	$\tau_f$ (ms)	$\tau_s$ at -130 mV (ms)
ACh	$0.13 \pm 0.03$ (9)	$4.2 \pm 0.4$ (9)
SubCh	$0.16 \pm 0.03$ (20)	$7.5 \pm 0.4$ (20)
DecCh	$0.3 \pm 0.1$ (3)*	$9.6 \pm 1.1$ (5)
CCh	$0.1 \pm 0.04$ (6)†	$1.3 \pm 0.1$ (10)

Time constants for the distribution of the burst length. Values of  $\tau_f$  are averaged over concentration and membrane potential. Values of  $\tau_s$  at -130 mV are from linear fits to  $\log \tau_s$  against  $E_m$  (all concentrations); the number of values is shown in parentheses.

\* In two out of five experiments with DecCh the faster component could not be defined.

† In four out of ten experiments with CCh the faster component could not be defined.

#### Voltage dependence of the frequency of channel activation

To determine the voltage dependence of the channel-opening reactions we measured the voltage dependence of the frequency of occurrence of 'long bursts' in three different membrane patches with 100 nm-SubCh in the pipette solution. To compensate for slow changes in the over-all rate of bursts the membrane potential was switched at 30 s intervals between the resting potential (-80 to -90 mV) and one of several more hyperpolarized test potentials, as indicated schematically in the upper part of Fig. 15. The number of long bursts in each 30 s interval was counted and plotted as a function of time (Fig. 15, graph). In order to avoid counting errors arising from the better resolution at the higher test potentials the analysis was restricted to bursts with durations longer than 0.5 ms. Fig. 15 illustrates the result of such an experiment, in which the membrane potential was switched between about -80 and -160 mV. The frequency of long bursts appeared to be slightly higher when the membrane potential was more hyperpolarized. The over-all burst frequencies at the two potentials were  $0.94 \text{ s}^{-1}$  at the resting potential, and  $1.28 \text{ s}^{-1}$  at a potential 80 mV more negative.

However, it is also obvious that with a sampling time of 30 s there are slow changes in the frequency of bursts which are not potential dependent. To compensate for these changes the frequency at a given test potential was normalized by expressing it as a fraction of the burst frequency measured in the 30 s intervals preceding and following the test potential. In this way we determined average burst frequencies at membrane potentials that were 40, 60 and 80 mV more negative than the resting potential. At the three more negative test potentials the burst frequencies (geometric means of  $n$  values) were increased by factors of  $1.13 \pm 0.09$  ( $n = 6$ ),  $1.25 \pm 0.10$  ( $n = 7$ ) and  $1.46 \pm 0.25$  ( $n = 5$ ) respectively, relative to the burst frequency at the resting

potential. However, the proportion of bursts that are omitted, because they are shorter than 0.5 ms, will be greater at the more positive potentials at which the burst duration is shorter. If we take the mean long-burst duration as 7.5 ms at  $-130$  mV (Table 2) and assume an e-fold lengthening for 70 mV hyperpolarization, then the

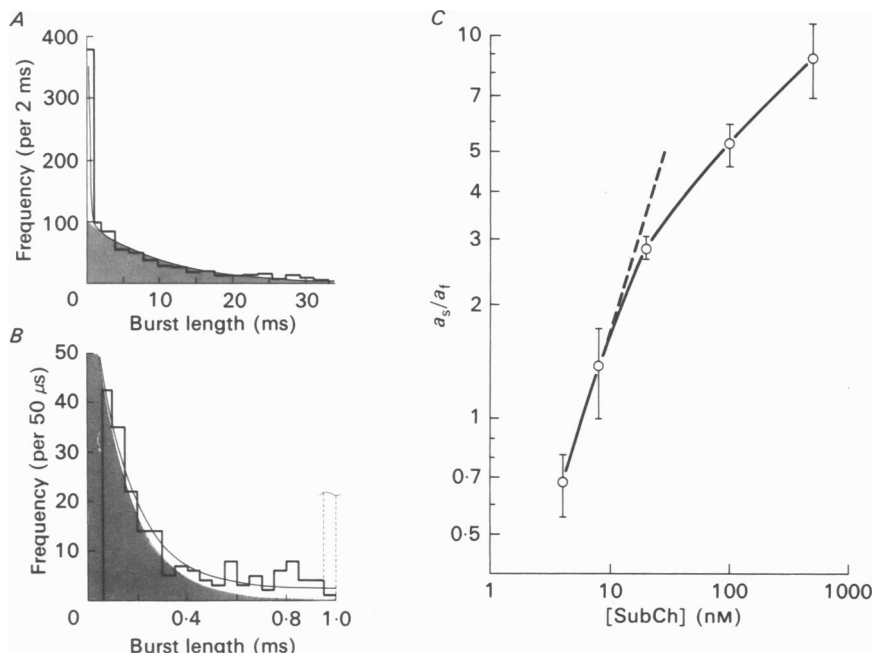


Fig. 14. The relative frequency of long bursts and short bursts as a function of the concentration for SubCh. An example of the distribution of the burst length for SubCh (20 nM,  $-131$  mV) is shown in A, and the part of this up to 1 ms is shown on an expanded scale in B. The area,  $a_s$ , that corresponds to the slower component is shaded in A, and the area,  $a_f$ , for the faster component is shaded in B. In this example  $a_f = 0.27$  and  $a_s = 0.73$  ( $\tau_f = 0.15$  ms,  $\tau_s = 10.2$  ms). In C, the relative area,  $a_s/a_f$ , is plotted against SubCh concentration in double logarithmic coordinates. The continuous line is drawn through the points by eye. The dashed line has a slope of unity and is drawn to fit the initial slope of the data.

frequency at  $-160$  mV (relative to that at  $-80$  mV) would be over-estimated by about 10 %. After correction for this effect the factors for  $\Delta V = 40$ , 60 and 80 mV become 1.06, 1.16 and 1.34 respectively. If this factor is assumed to depend exponentially on membrane potential then a fit to these results (constrained to go through a factor of unity at  $\Delta V = 0$ ) suggests that a hyperpolarization of  $350 \pm 90$  mV is needed to produce an e-fold increase in burst frequency. There appears to be a small but statistically significant voltage dependence.

#### *The mean open time and the mean number of openings per burst*

It is possible to estimate the number of short gaps that are missed by extrapolation of the distribution of shut times (e.g. Fig. 3) to zero time. The total open time (plus

unresolved gap time) can also be estimated by extrapolation of the burst length distribution. Therefore it is possible to estimate the *mean* length of a single opening, and the *mean* number of openings (or of gaps) per burst though the *distributions* of these quantities cannot be observed (see Methods, and Colquhoun & Sigworth, 1983).

The results obtained are presented in Table 3 for all agonists except CCh which is discussed separately below. The corrected mean open time is the total open time

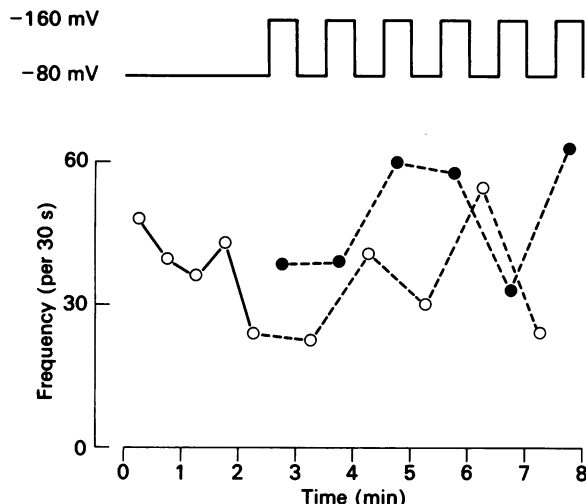


Fig. 15. Voltage dependence of the frequency of occurrence of (long) bursts. SubCh, 100 nM, 12 °C. The membrane potential was held initially for 9 min at about -80 mV (calculated from the amplitude of single-channel currents by taking the conductance as 30 pS). The patch-pipette potential was then stepped repeatedly between 0 mV and 80 mV (i.e. about -80 mV and -160 mV membrane potential). The time course of steps in pipette potential is indicated by the continuous line above the graph. ○, number of long bursts in each 30 s interval at -80 mV; ●, number of bursts at -160 mV. Each data point is drawn at the middle of the 30 s interval. The average rate of occurrence of bursts at -80 mV was  $0.98 \text{ s}^{-1}$ , and at -160 mV it was  $1.46 \text{ s}^{-1}$ . The small fast component of short bursts less than 500  $\mu\text{s}$  in duration was not taken into account. The mean burst lengths at the two potentials were 5.8 ms at -80 mV and 14.4 ms at -160 mV.

in a burst divided by the extrapolated total number of gaps within a burst plus 1, i.e. it is an estimate of what the mean length of a single opening would be if all brief gaps were resolvable. The mean number of short gaps per long burst (see Methods) is given because this is the parameter that seems most likely to have a simple physical significance (see Discussion); however, it differs only slightly from the number found if all bursts rather than long bursts are included, except at the lowest agonist concentrations where there are many short bursts. The absolute frequency of short gaps per unit open time is also given in Table 3; again the effect is small if all gaps are included (short and intermediate), or if the open time in long bursts is used in place of the total open time. The analogous quantities for the longer intermediate gaps are also shown in Table 3.

It may be noted that, for all agonists, the corrected mean open time is much longer

TABLE 3. Burst characteristics

Agonist	Corrected mean open time (ms)	Mean no. of short gaps per long burst		Mean no. of intermediate gaps per long burst		Mean no. of short gaps per unit open time ( $\text{ms}^{-1}$ )	Mean no. of intermediate gaps per unit open time ( $\text{ms}^{-1}$ )
		n	$\tau_t$ ( $\mu\text{s}$ )	n	$\tau_m$ (ms)		
ACh	1.4 ± 0.2 (10)	1.9 ± 0.2 (10)	39	0.86	3.1	0.56	0.014 ± 0.003 (8)
SubCh	1.6 ± 0.1 (19)	4.1 ± 0.3 (15)	38 ± 1.1	1.6 ± 0.2	5.6 ± 0.2	1.4 ± 0.1	0.019 ± 0.003 (21)
DeeCh	3.3 ± 0.6 (5)	2.0 ± 0.1 (5)	41	1.2	3.43	0.12	0.0052 ± 0.002 (4)

The values given in the first, fourth and fifth columns were potential dependent (to about the same extent as the slow component of the burst length distribution). The values given are those estimated from a semilogarithmic plot for a membrane potential of -130 mV. The number of determinations as given in parentheses.

TABLE 4. Burst characteristics in solutions with modified ion concentrations

Ion	Concn.	n	$\tau_t$ ( $\mu\text{s}$ )	$\tau_m$ (ms)	Mean number of gaps per long burst		Mean long burst duration (ms)	Single-channel conductance (pS)
					Short	Intermediate		
[H <sup>+</sup> ] <sub>o</sub>	pH 8.2	2	39	0.86	3.1	0.56	11.6	30
[Ca <sup>2+</sup> ] <sub>o</sub>	0.18 mM	4	38 ± 1.1	1.6 ± 0.2	5.6 ± 0.2	1.4 ± 0.1	4.7	44 ± 0.9
[Mg <sup>2+</sup> ] <sub>o</sub>	1.8 mM	1	41	1.2	3.43	0.12	6.7	29
[Cl <sup>-</sup> ] <sub>i</sub>	≈ 115 mM	2	38	1.6	3.4	0.14	6.4	31
*[Cl <sup>-</sup> ] <sub>i</sub>	115 mM	1	35	0.64	2.8	0.12	4.5	32

The number of experiments is denoted as n. The agonist was SubCh, 100 nM, in all experiments. The single-channel conductance was the slope conductance measured over a range of at least 60 mV around the resting potential. The two experiments at pH 8.2 were done at -130 mV and -170 mV membrane potential. All other experiments were at -100 mV to -130 mV. Two experiments with high [Cl<sup>-</sup>]<sub>i</sub> were done by Cl<sup>-</sup> loading (see text). A third (\*) was done with an inside-out patch. The normal concentrations were pH 7.2; [Ca<sup>2+</sup>]<sub>o</sub> = 1.8 mM; [Cl<sup>-</sup>]<sub>i</sub> ≈ 10 mM.

than the mean length of short bursts ( $\tau_f$  in Table 2), so it seems that short bursts are not simply isolated single openings of the type that occur in long bursts (this is discussed in detail later).

*Agonist dependence.* The corrected mean open time is rather similar for ACh and SubCh. The reason for the longer mean burst length for SubCh is primarily that it

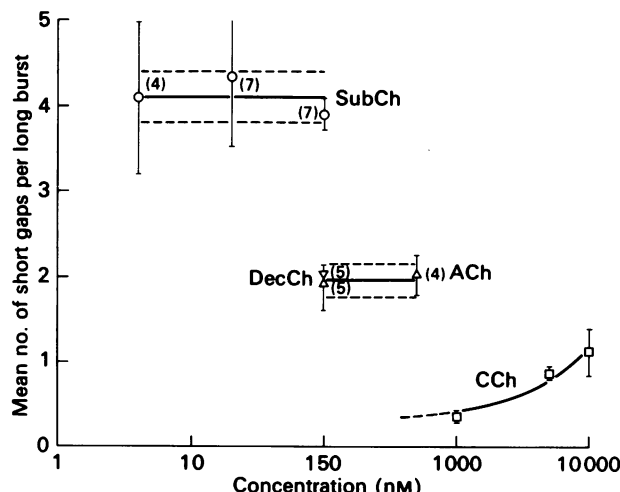


Fig. 16. The mean number of short gaps per long burst as a function of agonist concentration. The horizontal lines for SubCh and ACh ( $\Delta$ ) represent the over-all mean values, and the dashed lines show their standard errors. The values for CCh have been corrected to a membrane potential of  $-170$  mV and the line drawn through them corresponds to a linear fit in arithmetic coordinates (see text).

has more openings per burst than ACh, the number of short gaps per unit open time being similar for both agonists. On the other hand, the reason that DecCh has a longer mean burst length than ACh is primarily because the length of individual openings is longer, the number of openings per burst being very similar to that for ACh. There are, of course, far fewer of the longer intermediate gaps. The numbers in Table 3 suggest that for each agonist there is one intermediate gap for every thirty or forty short gaps.

*Concentration dependence.* None of the quantities in Table 3 showed an unambiguous dependence on agonist concentration over the range tested, except for CCh which is discussed separately below. For measurements at membrane potentials near  $-130$  mV the correct mean open times for SubCh were: at  $4$  nM,  $1.5 \pm 0.2$  ms ( $n = 3$ ); at  $20$  nM,  $1.3 \pm 0.3$  ms(3); at  $100$  nM,  $1.5 \pm 0.3$  ms(5); at  $500$  nM,  $2.8 \pm 0.5$  ms(3). For ACh at  $100$  nM we found  $1.5 \pm 0.2$  ms(4); at  $500$  nM,  $1.3 \pm 0.1$  ms(3). The number of gaps per unit open time at potentials near  $-130$  mV for SubCh were: at  $4$  nM,  $0.4 \pm 0.1$  ms $^{-1}$ (3); at  $20$  nM,  $0.7 \pm 0.1$  ms $^{-1}$ (3); at  $100$  nM,  $0.6 \pm 0.1$  ms $^{-1}$ (5); at  $500$  nM,  $0.3 \pm 0.02$  ms $^{-1}$ (3). For ACh the values were: at  $100$  nM,  $0.4 \pm 0.1$  ms $^{-1}$ (5); at  $500$  nM,  $0.5 \pm 0.1$  ms $^{-1}$ (3).

The number of short gaps per long burst is plotted against agonist concentration

in Fig. 16. No dependence on concentration is seen for SubCh or ACh, but the number of gaps per burst increases with CCh concentration (see below).

There was some indication of an increased open time at 500 nM-SubCh but this cannot be regarded as reliable because of the modest number of observations and because of the less certain definition of bursts at higher agonist concentrations.

*Voltage dependence.* The results with agonists other than CCh were all similar. The mean open lifetime showed a voltage dependence similar to that of the mean burst length (slow component,  $\tau_s$ ). A semilogarithmic fit indicated that a hyperpolarization of  $54 \pm 8$  mV for SubCh, and  $60 \pm 19$  mV for ACh, produced an e-fold lengthening. Thus it would be expected that the number of gaps per burst (and hence the number of openings per burst) would not depend on membrane potential, and indeed no significant dependence was observed for SubCh, ACh or DecCh, the slope of the semilogarithmic plot for SubCh being  $(4 \pm 30) \times 10^{-4}$  mV<sup>-1</sup>. The mean number of gaps per unit open time, as expected from the foregoing observations, was found to decline e-fold for a  $56 \pm 11$  mV hyperpolarization for SubCh, and for  $69 \pm 30$  mV for ACh.

#### *Results with carbachol*

Fig. 16 showed that CCh behaved differently from the other agonists in that the number of short gaps per long burst decreased at low agonist concentrations. The gap length distributions were fitted with three exponentials in the usual way, and the same results were also fitted with the time constant of the fast component,  $\tau_f$ , constrained to be 14  $\mu$ s; the latter procedure was used in order to increase the precision of the estimate of the relative areas which was difficult to estimate especially at 1  $\mu$ M-CCh where very few gaps could be seen (e.g. in one case 1534 gaps were measured; after imposition of a resolution of 60  $\mu$ s for openings and 40  $\mu$ s for gaps there were 1379 gaps to be fitted, and of these about 16 were short gaps and 12 were intermediate gaps).

The corrected mean number of short gaps per long burst were, from constrained fits,  $1.2 \pm 0.4$  ( $n = 3$ ) with 10  $\mu$ M-CCh,  $0.58 \pm 0.12$  ( $n = 4$ ) with 5  $\mu$ M-CCh and  $0.19 \pm 0.04$  ( $n = 3$ ) with 1  $\mu$ M-CCh; similar values were observed with unconstrained fits. Moreover, contrary to what was seen with other agonists, the mean number of gaps per burst with CCh appeared to be voltage dependent, showing an e-fold increase for roughly 70 mV hyperpolarization (though the data did not allow very precise estimation of this). The values plotted in Fig. 16 have been corrected to a membrane potential of -170 mV on this basis, and show a similar, but rather less pronounced, concentration dependence. The mean number of short gaps per burst increases roughly linearly with CCh concentrations with a slope of  $(8.3 \pm 2.5) \times 10^4$  M<sup>-1</sup>, and a zero concentration intercept of  $0.34 \pm 0.16$  at -170 mV (this line is plotted in Fig. 16 on semilogarithmic coordinates). When converted to -130 mV the slope was  $(4.7 \pm 1.4) \times 10^4$  M<sup>-1</sup> and the intercept  $0.19 \pm 0.09$ . Similarly, the mean number of short gaps per unit open time (from constrained fits) increased with concentration with a slope of  $(4.2 \pm 1.3) \times 10^7$  M<sup>-1</sup> s<sup>-1</sup>; no voltage dependence was detectable.

These results strongly suggest that in the case of CCh, unlike all the other agonists tested, most of the short gaps result from ion-channel block (see also Ogden & Colquhoun, 1985). The quantitative aspects of this conclusion are considered in the Discussion. The intercept at zero concentration suggests that there may be some short

gaps that do not result from channel block; if so, there are probably fewer than 0.3 per long burst and they are presumably comparable in length to the blockages.

The mean length of the intermediate gaps for CCh was  $0.13 \pm 0.03$  ms. The number of intermediate gaps per long burst was  $0.024 \pm 0.006(10)$ , and the number per millisecond of open time was  $0.015 \pm 0.004(10)$ . The precision of the data was insufficient to reveal any dependence on concentration or membrane potential in these quantities.

#### *Effects of changing ionic composition*

At the normal resting potential of the muscle fibre the current through the open end-plate channel is carried predominantly by  $\text{Na}^+$  flowing into the cell. Brief interruptions of the single-channel current, as illustrated in Figs. 1 and 11, could be caused by a mechanism related to  $\text{Na}^+$  transport through the channel, for example blockage of the open channel by other cations. To investigate this possibility we have determined the mean duration and frequency of the brief current interruptions in solutions of various ionic compositions, both on the extra- and intracellular side of the membrane. Otherwise standard conditions (100 nM-SubCh and membrane potentials of  $-100$  to  $-180$  mV) were maintained. The ion composition of the extracellular solution was modified in such a way that a blocking effect of external cations from the extracellular side should be reduced. We thus reduced the concentrations of  $\text{H}^+$  or of  $\text{Ca}^{2+}$  in the pipette solution. On the other hand, blockage could also be caused by large intracellular ions or by some unknown substance. This possibility was investigated by measuring single-channel currents in a well defined medium, with a  $\text{Cl}^-$  concentration of 115 mM, on the intracellular side.

#### *Reduction in extracellular $[\text{H}^+]$*

It has been shown that the ACh-evoked conductance at the frog end-plate is dependent on the pH of the extracellular solution. When extracellular pH is lowered from the normal value of pH 7.2 the conductance decreases and increases with higher than normal pH (Scuka, 1977; Landau, Gavish, Nachshen & Lotan, 1981). Comparable effects have been observed in avian muscle and have been shown to be at least partially caused by an apparent reduction in single-channel current amplitude by  $\text{H}^+$ ; these effects have been attributed to blocking of the channel by  $\text{H}^+$  (Landau *et al.* 1981; Goldberg & Lass, 1983). Since protonation and deprotonation of proteins can occur in the time range of tens of microseconds (Hammes, 1979) it is a possibility that the brief interruptions of single-channel currents observed at pH 7.2 could be blockages of the end-plate channel by  $\text{H}^+$ . However, a 10-fold reduction in extracellular  $[\text{H}^+]$  did not alter the burst characteristics of end-plate channels. Both the mean duration and the mean number of short gaps per long burst, in two experiments performed at pH 8.2, were within the range of the mean values found at the normal pH (7.2), as shown in Table 4. Therefore channel block by  $\text{H}^+$  seems an unlikely mechanism for the short interruptions.

#### *Reduction in extracellular $[\text{Ca}^{2+}]$*

It is known that  $\text{Ca}^{2+}$  can permeate the end-plate channel, though at a very much lower rate than monovalent metal cations (Bregestowski, Miledi & Parker, 1979;

Lewis, 1979). It is also known that the permeability of the end-plate channel for monovalent cations is reduced when extracellular  $[Ca^{2+}]$  is raised (Adams, Dwyer & Hille, 1980). This effect has been attributed to a decrease in the density of negative surface charges (Lewis, 1979; Adams *et al.* 1980). However, the reduced permeability could also result from occupancy by  $Ca^{2+}$  of the channel site for permeating cations (Marty, 1980), so the short current interruptions could be caused by brief blockages by  $Ca^{2+}$ . We therefore examined single-channel end-plate currents with extracellular solutions in which the  $[Ca^{2+}]$  was reduced from 1.8 to 0.18 mM.

Two effects of a reduced extracellular  $[Ca^{2+}]$  were obvious. First, the amplitude of single-channel currents at the resting potential was increased by 50%. This was due to an increase in the slope conductance, which was increased to  $44 \pm 0.9$  pS, as compared to 29 pS in our control conditions (see also Anderson & Stevens, 1973; Lewis, 1979; Gardner, Ogden & Colquhoun, 1984). Secondly, single-channel currents have more interruptions than in solutions with normal  $[Ca^{2+}]$  (1.8 mM). The burst analysis of single channel currents recorded with low extracellular  $[Ca^{2+}]$  shows that the mean duration of both the short and the intermediate gaps is much the same as in control conditions. However, the number of gaps of intermediate duration per long burst is increased nearly 10-fold (Table 4).

In one experiment extracellular  $Ca^{2+}$  was replaced by 1.8 mM- $Mg^{2+}$ . The slope conductance and the burst characteristics found in this experiment were in the range obtained with 1.8 mM- $Ca^{2+}$ . It thus appears that both the increase in slope conductance, and the increased number of intermediate duration gaps per burst, observed in low  $[Ca^{2+}]$  solutions are not specific for a reduction in extracellular  $[Ca^{2+}]$ . Rather they are due to the reduced concentration in extracellular divalent cations.

Whatever the precise mechanism of the effects of divalent cations on conductance and gating of end-plate channels may be (see Discussion), the fact that the number of gaps per long burst is not reduced by lowering extracellular  $[Ca^{2+}]$  argues against the current interruptions being caused by channel block by permeating  $Ca^{2+}$ .

#### *Increase in intracellular $[Cl^-]$*

Brief gaps could also result from channel block from the intracellular side by some intracellular molecule or ion. At -90 mV membrane potential  $Cl^-$  is close to electrochemical equilibrium. However, at the more negative membrane potentials of -130 mV, where most experiments were performed,  $Cl^-$  could possibly block the end-plate channel on the intracellular side. In order to investigate channel blocking by intracellular  $Cl^-$  we have made measurements in preparations with increased intracellular  $[Cl^-]$ . Muscles were immersed in isotonic (115 mM) KCl for several (more than 2) hours. Due to the high  $Cl^-$  permeability of skeletal muscle, this treatment increases the intracellular  $[Cl^-]$  to close to the extracellular concentration of 115 mM (Boyle & Conway, 1941). The two measurements made at -100 mV membrane potential in these conditions gave results which are comparable to those seen in control conditions (Table 4).

Finally, current interruptions could be caused by some unknown intracellular constituent which blocks channels from inside. To check this possibility one measurement was made on an isolated, inside-out membrane patch with 115 mM-KCl and 0.5 mM-EGTA (at pH 7.2) on the cytoplasmic side of the membrane patch. In this

experiment the mean duration of current interruptions and the mean number of interruptions per burst were within the range found in control conditions (Table 4). These results make it unlikely that channel blocking by any soluble molecule from the cytoplasmic side could account for the brief gaps.

#### *Distributions based on apparent open times*

Although the measured open times (apparent open times) are merely the lengths of partially resolved bursts, they may nevertheless contain useful information. One can, for example, ask the following questions. (a) Are bursts homogeneous in the sense that long and short bursts are made up of similar apparent openings? (b) What is the distribution of the number of apparent openings per burst, and of the lengths of bursts with a specified number of apparent openings? (c) Do short bursts contain any detectable gaps (if not, they might more appropriately be called short openings)? (d) Do short openings occur as part of long bursts (knowledge of this would cast light on the relationship, if any, between the putative two sorts of open state)?

The distribution of the apparent open time is not expected to be described by a sum of exponentials, though in some cases a sum of exponentials may be a close approximation to the expected form (A. G. Hawkes & D. Colquhoun, in preparation). The case of the number of apparent openings per burst is, however, a bit simpler because, even when many gaps are undetected, this distribution is still expected to have the form of a sum of geometric components, the number of components being equal to the number of open states (as is the case when resolution is not limited; Colquhoun & Hawkes 1982, 1983). The means of these components will, of course, be affected by the limited resolution, e.g. the mean number of apparent openings per burst (see Fig. 17) will be smaller than the mean number of openings per burst given in Table 3 because the latter have been corrected for undetected gaps.

#### *The distribution of the number of apparent openings per burst*

This can also be described as the distribution of the number of resolved gaps per burst because the number of apparent openings in a burst is necessarily one greater

---

Fig. 17. Distribution of the total open time per burst (left-hand column) fitted with two exponentials (continuous line), and of the number of apparent openings per burst (right-hand column) fitted with two geometrics (dashed line). Distributions are shown for SubCh at concentrations of 4 nm (top row), 20 nm (middle row) and 100 nm (bottom row). The area for each component is given in parentheses after the time constant. A, SubCh, 4 nm. Membrane potential -188 mV. Critical gap length for definition of bursts 3 ms. The exponentials have time constants of  $0.16 \pm 0.02$  ms ( $68.6 \pm 3.2\%$ ) and  $22.8 \pm 3.9$  ms ( $31.4 \pm 3.2\%$ ). The inset shows the short end of this distribution on an expanded scale (up to 1 ms), to display the time constant of 0.16 ms more clearly. The geometrics have means of  $1.08 \pm 0.07$  ( $71 \pm 13\%$ ) and  $2.64 \pm 0.90$  ( $29 \pm 13\%$ ). B, SubCh, 20 nm. Membrane potential -131 mV. Critical gap length 2 ms. The exponentials have time constants of 0.12 ms (29.8%) and 8.8 ms (70.2%). The geometrics have means of  $1.05 \pm 0.14$  ( $27 \pm 12\%$ ) and  $2.23 \pm 0.24$  ( $73 \pm 12\%$ ). C, SubCh, 100 nm. Membrane potential -123 mV. Critical gap length 3 ms. In the exponential fit, the faster time constant was constrained to 0.16 ms to facilitate the estimation of its small area (13%). The longer time constant was 8.0 ms (87%). The geometrics have means of 1.16 (13%) and 2.02 (87%) but the relative areas are poorly defined in this case.

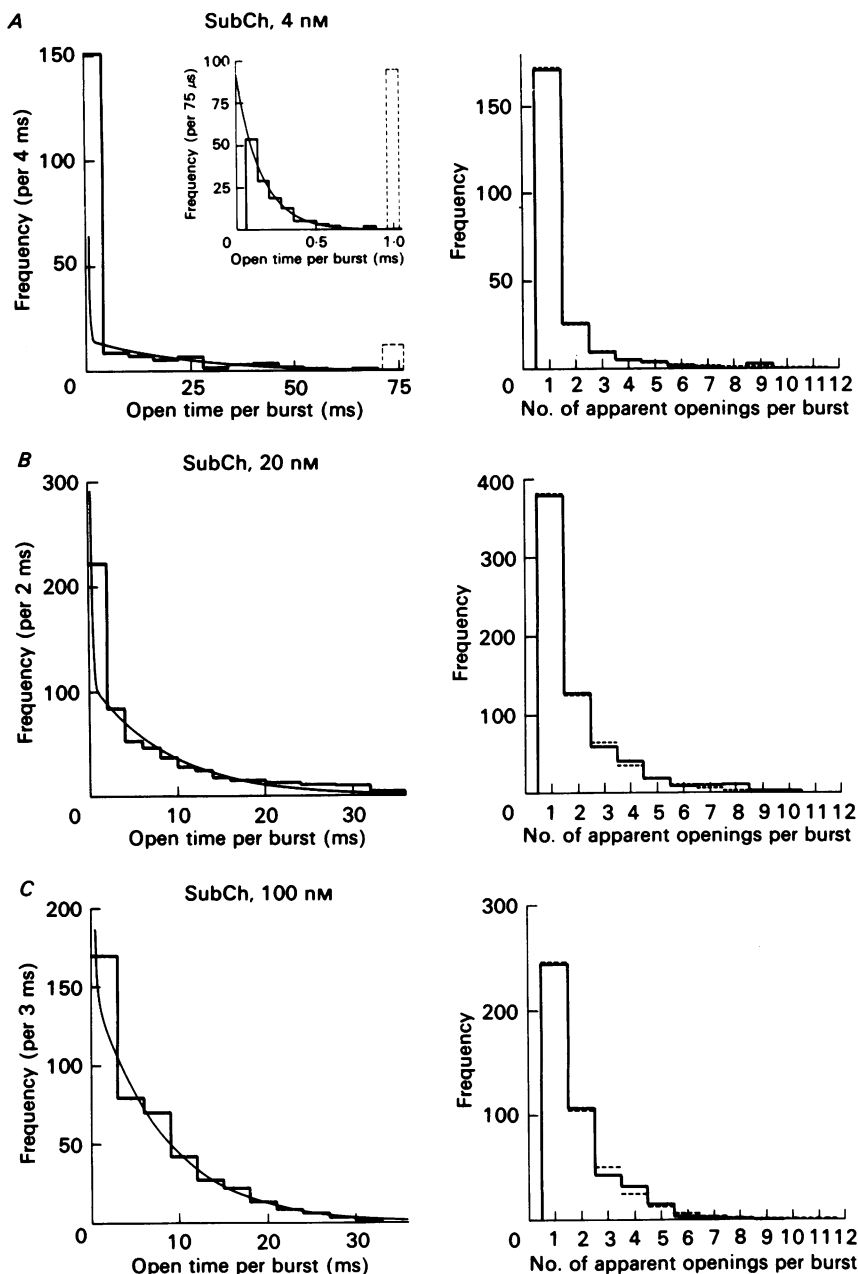


Fig. 17. For legend see opposite.

than the number of gaps that are detected. In some cases a simple geometric distribution provided an adequate fit of the data, but often, especially at low agonist concentrations, a mixture of two geometrics was required (as might be expected in view of the evidence already adduced for there being two open states), i.e. the

probability of  $r$  apparent openings (or  $r-1$  detected gaps) per burst can be written in the form (Colquhoun & Sigworth, 1983)

$$P(r) = a_1\mu_1^{-1}(1-\mu_1^{-1})^{r-1} + a_2\mu_2^{-1}(1-\mu_2^{-1})^{r-1}, \quad (11)$$

where  $a_1, a_2$  are the areas of the two components ( $a_1 + a_2 = 1$ ) and  $\mu_1, \mu_2$  are the means of the components. Fig. 17 shows examples of these distributions obtained with three different concentrations of SubCh. In each case there is a component with a mean,  $\mu_1$ , close to unity, and a second component with a larger mean (the exact value will depend on the number of undetected gaps, i.e. on the resolution of the experiment). The existence of a component with unit mean implies, loosely speaking, that there is a component of bursts that have only one apparent opening per burst, i.e. no detected gaps in the burst.

This case is of particular interest because it can be shown (A. G. Hawkes & D. Colquhoun, in preparation) that the existence of a component with unit mean in the presence of limited resolution usually implies that there is a component of unit mean in the 'true' distribution of the number of openings per burst that would be found if all short gaps were detected (i.e. roughly speaking, gaps cannot be missed if there are no gaps). Thus the observations suggest that even with better resolution the distribution would still have a component with unit mean, though the second component of the distribution would have a mean substantially greater than that observed here.

#### *The characteristics of bursts with a fixed number of apparent openings*

The observations in Fig. 17 showed that the component with unit mean is more prominent (has a larger area) at low SubCh concentrations (at which, it has already been shown, there is a larger proportion of short bursts). This suggests (but does not itself show) that the short bursts do not usually contain gaps (in which case they might

Fig. 18. The distribution of all apparent open times (*A*), and of the total open time per burst for bursts with 1–5 apparent openings (*B–F*). SubCh, 100 nM. Membrane potential –161 mV. The critical gap length for definition of bursts was 2.5 ms (the time constants for the distribution of all shut periods were 39.8 µs, 0.52 ms and 339 ms; see Fig. 11 and eqn. (3)). Resolution was set to 60 µs for openings and 50 µs for shut periods. Time spent in sublevels was counted as part of the open time. *A*, the distribution of the duration of all apparent openings. Fit of 782 values between 0.06 and 30 ms with two exponentials gave time constants of 0.18 ms (7.3%) and 10.2 ms (92.7%). Predicted total number of events = 845.3. *B*, distribution of the duration of bursts that contain only one apparent opening. Fit of 255 values between 0.06 ms and 50 ms with two exponentials gave time constants of 0.17 ms (17.1%) and 10.1 ms (82.9%). Predicted total number of events = 271.9. *C*, distribution of the total open time per burst for 81 bursts with  $k = 2$  apparent openings. The line shows the maximum likelihood fit of the gamma distribution,  $\Gamma_2(t)$  (see Methods). The mean,  $k\tau_o$ , was 21.2 ms, so  $\tau_o = 10.6$  ms which is similar to the mean length of the long apparent openings found in *A* and *B*. *D*, distribution of total open time per burst for 43 bursts with  $k = 3$  apparent openings. The fitted  $\Gamma_3(t)$  distribution has a mean,  $k\tau_o$ , of 33.9 ms, so  $\tau_o = 11.3$  ms. *E*, distribution of total open time per burst for 32 bursts with  $k = 4$  apparent openings. The fitted  $\Gamma_4(t)$  distribution has a mean of 51.6 ms, so  $\tau_o = 12.9$  ms. *F*, distribution of total open time per burst for 14 bursts with  $k = 5$  apparent openings. The fitted  $\Gamma_5(t)$  distribution has a mean of 57.0 ms, so  $\tau_o = 11.4$  ms.

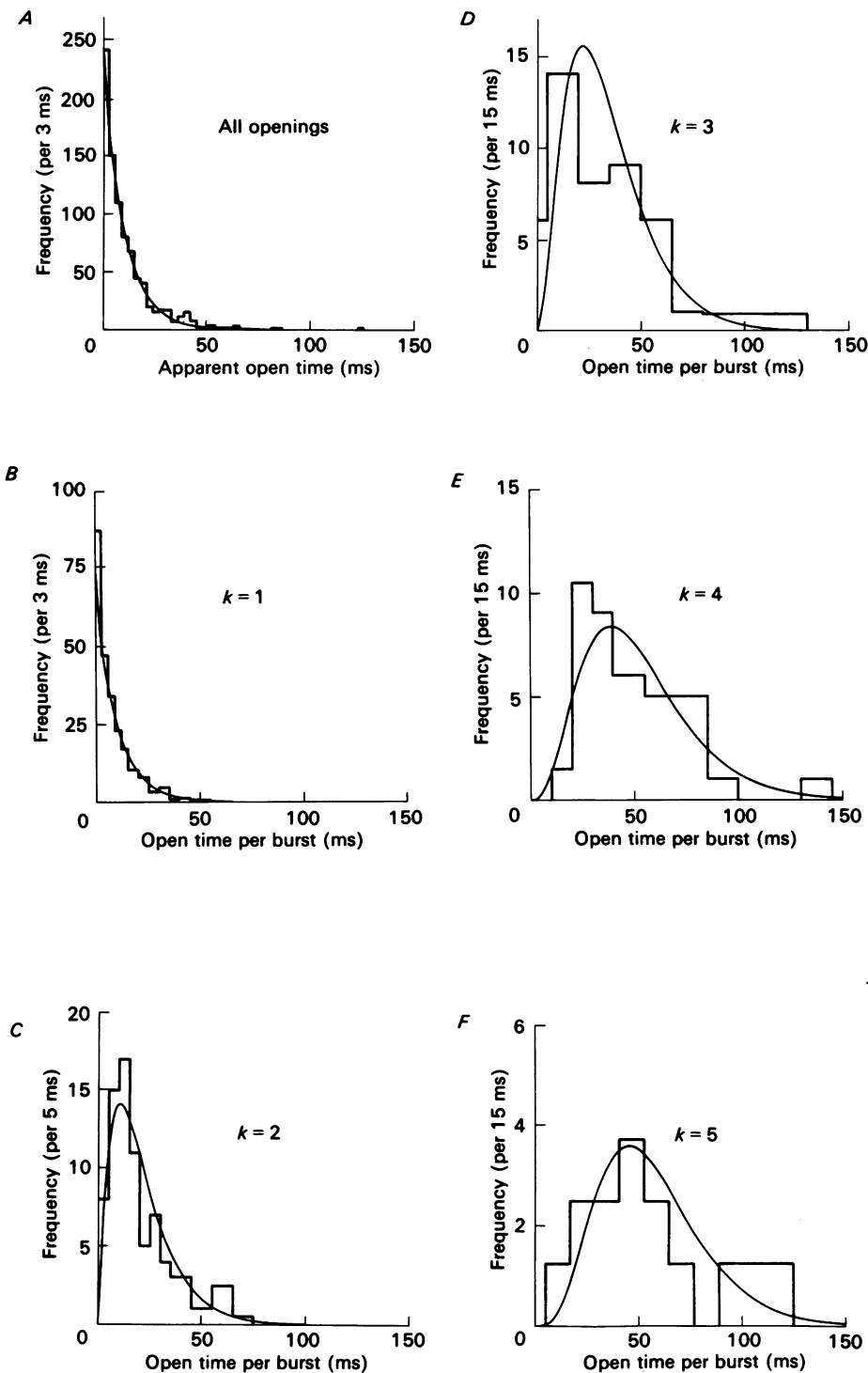


Fig. 18. For legend see opposite.

more appropriately be called short openings). This conclusion can be tested by comparison of the distribution of all apparent open times, exemplified in Fig. 18A, with the distribution of the lengths of bursts that contain only one apparent opening, which is exemplified in Fig. 18B. The time constants for the fast and slow components are very similar for both distributions, but the fast component makes up a *larger proportion* of the area for the latter. The area of the fast component in Fig. 18A suggests that there are about 60 short bursts altogether, and the area under the fast component in Fig. 18B suggests that most (47) of these did indeed occur as single openings, i.e. they contained no detectable gaps. If this is the case then bursts with *more* than one apparent opening should contain few short openings.

This question is investigated in Fig. 18C–F, which show separately the distributions of the total open time per burst (which is approximately the same as the burst length) for bursts that contained 2–5 apparent openings. These distributions also bear on the question of whether bursts with many apparent openings are made up of the same sort of openings as bursts with few apparent openings. Suppose that all bursts with more than one apparent opening are made up of a series of apparent openings of exponentially distributed length with a mean length,  $\tau_o$ , equal to that of the slow component (the long openings) in the distribution of all apparent open times (i.e.  $\tau_o = 10.2$  ms in Fig. 18A). The open time per burst for bursts with  $k$  openings should then follow a gamma ( $\Gamma_k$ ) distribution with mean  $k\tau_o$ . The distributions in Fig. 18C–F have been fitted with  $\Gamma_k(t)$  probability density functions, as described in the Methods. The fits are reasonably good, and it can be seen from the values given in the legend to Fig. 18 that the mean open time per burst in bursts with 2–5 apparent openings are indeed, to a good approximation, integer multiples of about 10.2 ms. Bursts are therefore, in this sense, homogeneous. They also appear to contain few short openings, though it must be stressed that unambiguous detection of short openings within a burst is not easy, as was illustrated in Fig. 8.

#### *Dependence of the mean apparent open time and mean gap length on position within the burst*

If all bursts are included, then the first apparent opening in a burst is shorter on average than subsequent openings, especially at low agonist concentration. This is expected because of the occurrence of isolated short openings.

If bursts with only one apparent opening are excluded, then the mean,  $m_2$  say, of the length of apparent openings in all other bursts (those with two or more apparent openings) is, as expected from the results already presented, similar to the time constant of the slow component in the distribution of all apparent open times. The mean length of an apparent opening in bursts with two or more apparent openings showed little sign of any consistent dependence on position within the burst. The only possible exception was that the first apparent opening in such bursts for SubCh may have been a little shorter than others, being  $92 \pm 3\%$  of  $m_2$  (ten experiments with 4–100 nm-SubCh, involving 1377 bursts with two or more apparent openings). For ACh (four experiments with 100 and 500 nM-SubCh) the mean length of apparent openings as a percentage of  $m_2$  was, for the first apparent opening  $98 \pm 4\%$  (excluding bursts with only one apparent opening), for the second  $99 \pm 4\%$ , for the third  $103 \pm 6\%$ , for the fourth  $115 \pm 10\%$ , and for the fifth  $102 \pm 15\%$ .

The mean length of gaps within bursts also showed no clear dependence on the position of the gap within the burst for any agonist. For example, for ACh (100–500 nM) the mean lengths as a percentage of the mean length of all gaps within bursts are, for the first gap  $103 \pm 4\%$ , for the second  $98 \pm 6\%$ , for the third  $93 \pm 10\%$ , and for the fourth  $90 \pm 15\%$ .

*Bursts with a fixed number of apparent openings.* Again no clear dependence on position within the burst was detected. For example in ACh-evoked bursts with three apparent openings the mean lengths of the first, second and third apparent openings, as a percentage of  $m_2$ , were  $101 \pm 8\%$ ,  $99 \pm 8\%$  and  $107 \pm 8\%$ , respectively. For ACh-evoked bursts with four apparent openings the mean lengths of the first, second and third gaps, as a percentage of the mean length of all gaps within bursts, were  $105 \pm 13\%$ ,  $108 \pm 13\%$  and  $94 \pm 14\%$  respectively. The lack of asymmetry in these numbers is compatible with mechanisms that obey the principle of microscopic reversibility (see, for example, Colquhoun & Hawkes 1982, 1983; Läuger, 1983); the test of this is, however, imperfect because the existence of undetected short gaps means, for example, that if there was an undetected gap before the first detected gap, then the first, second and third (detected) gaps referred to above would actually be the second, third and fourth gaps.

#### *Openings on each side of intermediate gaps*

Gaps within bursts were classified into short and intermediate types according to whether they were shorter or longer than a specified duration,  $t_c$ , chosen as described in the Methods (eqn. (3)). With average values (Table 1)  $t_c$  would be about 50  $\mu s$  for ACh (giving 9 % misclassification), and 106  $\mu s$  for SubCh (giving 8 % misclassification). The other criteria mentioned in the Methods would suggest longer  $t_c$  values but would misclassify 18–24 % of long intervals, though the absolute number of misclassifications would be smaller. The mean lengths of the apparent openings which preceded and followed each intermediate gap were measured. With SubCh (ten experiments, 4–100 nM, 1238 gaps) the length of the preceding apparent opening as a percentage of  $m_2$  was  $96 \pm 3\%$  and that of the following opening was  $106 \pm 3\%$ . Therefore both preceding and following openings were typical long openings, with a hint that the preceding openings might be slightly shorter. The results for ACh and DecCh were similar.

#### *Correlations of apparent open times and of burst lengths*

Correlations between the length of an event and length of a later event can provide information about the number of pathways that link the open and closed states (see Discussion). Measurements of the number of runs and of autocorrelation coefficients were made (see Methods). Two problems interfere with these measurements: (a) lack of knowledge of the number of channels in the patch, and (b) undetected short gaps (see Discussion).

*Correlation of apparent open times.* Correlations were clearly detectable only at the lowest concentration (4 nM) of SubCh that was tested. The runs test, with a critical time of 0.3 ms (see Methods), gave a standard Gaussian deviate of  $z = -7.1$  (pooled value from four experiments). This is strong evidence for the existence of runs of ‘short’ (less than 0.3 ms) and ‘long’ apparent openings. The autocorrelation co-

efficient with lag 1 (see Methods) for apparent open times in these experiments was  $r_1 = 0.066$  (95% confidence limits 0.014–0.12); likewise  $r_2 = 0.068$  (0.015–0.12) and  $r_3 = 0.029$  (−0.023 to 0.082). As might be expected, the correlation was most pronounced in the experiment with the best resolution (60  $\mu$ s for openings, 40  $\mu$ s for gaps) which gave  $z = -4.2$  for the runs test, and autocorrelations of  $r_1 = 0.15$  (0.05–0.24),  $r_2 = 0.10$  (0.00–0.20) and  $r_3 = 0.024$  (−0.08 to 0.12).

At SubCh concentrations of 20 nM and greater, correlations could not be detected with any certainty; the runs test gave  $z = -0.40$  (eight experiments). Similarly ACh (100 nM) gave  $z = -1.0$  and  $r_1 = 0.021$  (−0.03 to 0.070) and DecCh (100 nM) gave  $z = -0.7$  and  $r_1 = 0.002$  (−0.03 to 0.04).

*Correlation of burst lengths.* No correlations could be detected for any concentration of any agonist. For example four experiments with SubCh (4 nM), which showed a correlation between apparent open times, gave for the burst length: (a) runs test  $z = -1.0$ , (b) autocorrelation  $r_1 = 0.001$  (−0.06 to 0.08).

*Correlations within bursts.* The correlation,  $r_{1j}$  say, between the length of the first and the  $j$ th apparent opening in a burst was calculated. For the lowest SubCh concentration (4 nM)  $r_{12} = 0.26$  (0.13–0.38) but  $r_{13}$  did not differ significantly from zero, as was also the case for  $r_{12}$  at higher SubCh concentrations. For ACh (100–500 nM) there may have been a small positive correlation too,  $r_{12} = 0.066$  (−0.01 to 0.14), though it is of marginal statistical significance.

## DISCUSSION

Our main object is to consider what sorts of mechanism might underlie the behaviour reported in the Results section.

### *The number of states*

If we suppose that the channel can exist in several more-or-less discrete states, that it is ‘memoryless’ and that the rate constants for transitions between states are constant (do not vary with time), then the number of shut states must be at least the number of exponential components that are needed to fit distribution of all shut times (Colquhoun & Hawkes, 1981, 1982). We therefore infer that there are at least three sorts of shut state. In addition, there are ‘desensitized’ states and blocked states which will not be discussed here; at high agonist concentrations two more exponentials are needed to account for putative desensitized states, and a sixth exponential for channel block (Sakmann, Patlak & Neher, 1980; Colquhoun & Sakmann, 1983; Sine & Steinbach, 1984*b*; Ogden & Colquhoun, 1985).

Similarly the number of open states can be inferred from the number of components fitted to the distribution of open times (or, more safely in the present case where we can measure only ‘apparent openings’, the distribution of total open time per burst; see Fig. 17). Thus it appears that there are at least two sorts of open state. We shall therefore proceed on the basis of three shut and two open states, though this could be wrong (a) if the assumptions are wrong (they are the usual Markov assumptions that underlie Law of Mass Action calculations, but there is little direct evidence for them), or (b) if the observed distributions were distorted for some reason so that it was not genuinely multi-exponential (e.g. because of limited frequency resolution,

A. G. Hawkes & D. Colquhoun, in preparation); in this case if a multi-exponential fit was attempted it could give rise to a misleading estimate of the number of components needed.

#### *The nature of the shut states*

Any postulate concerning the physical nature of the state(s) that are occupied during the brief gaps, or the much rarer intermediate gaps, within bursts must take into account the following observations: (a) the mean duration of the gaps within bursts is clearly dependent on the nature of the agonist, and (b) neither the mean duration nor the frequency of such gaps is very dependent on either agonist concentration or on membrane potential (except for CCh).

#### *Normal shut channels*

There is now abundant biochemical evidence that there are two binding sites for agonist per ion channel (see, for example, Karlin, Cox, Kaldany, Lobel & Holtzman, 1983). This is consistent with electrophysiological evidence concerning the co-operativity of the response. Therefore it is clear that there must be at least three shut states of the normal channel (those with 0, 1 and 2 agonist molecules bound). Gaps within bursts could be caused by oscillation between the open state(s) and the shut (but occupied) states, as suggested by Colquhoun & Hawkes (1977). It is not, however, self-evident that these three normal shut states correspond to the three shut states that we infer from our results. If, for example, the binding reactions that link these three states occurred very rapidly on the time scale of our observations (as proposed by Anderson & Stevens, 1973) the three states would be kinetically indistinguishable. There are certainly other possible explanations for the shut states that we have observed. Some of these will now be discussed.

#### *Ion channel blockages by the agonist*

An obvious possibility is that brief gaps might be caused by transient blockages of the open ion channel by the agonist itself. The lack of agonist-concentration dependence in the frequency of short and intermediate shut periods seen with ACh and SubCh rules out the possibility that these shut periods result from block by the agonist molecules themselves. On the other hand, our results do suggest that the brief gaps seen with CCh are the result of ion-channel block by the agonist. The characteristics of channel block produced by these compounds has been determined, on the same preparation, by Ogden & Colquhoun (1985) (see also Sine & Steinbach, 1984*b*, for similar experiments on the BC3H-1 cell line). These experiments suggest that blockages produced by ACh molecules have a mean duration of about 18  $\mu$ s, which is very similar to the mean duration of the brief gaps (20  $\mu$ s) seen here with ACh. However, at the highest ACh concentrations used here (500 nM) there should be only 0.018 blockages per millisecond of open time whereas we have observed far more, viz. 0.46 brief gaps per millisecond of open time (a value that is very similar for both 100 and 500 nM-ACh). Ogden & Colquhoun (1985) also found that channel blockages by SubCh have a mean duration of about 5 ms, and should occur at 0.004 per millisecond of open time at 100 nM-SubCh whereas we observe brief gaps of 43  $\mu$ s mean duration at 0.47 per millisecond of open time. It is likely that DecCh also produces channel blockages that are far longer than the 71  $\mu$ s short gaps seen here,

as judged by the slow inverse relaxation that follows a hyperpolarizing voltage jump in the Vaseline-gap voltage clamp (D. J. Adams & D. Colquhoun, unpublished observations).

*Results with carbachol.* We have found that with CCh, unlike the other agonists, the number of short gaps per burst increases with agonist concentrations. If this effect is interpreted as channel block by CCh, the unblocking rate constant would be  $1/13.2 \mu\text{s} = 7.6 \times 10^4 \text{ s}^{-1}$  at 130 mV. The association rate constant for blockage of open channels can be estimated from the concentration dependence of the number of blockages per burst (slope  $4.7 \times 10^4 \text{ M}^{-1}$  at -130 mV). For a simple open-channel blocker this can be divided by the mean total open time per activation in the absence of block (taken as the time constant for the slow component of the burst length distribution, i.e. 1.3 ms from Table 1); this gives an association rate constant of  $3.6 \times 10^7 \text{ M}^{-1} \text{ s}^{-1}$  at -130 mV. The same quantity can also be estimated from the slope of the plot against concentration of the mean number of blockages per unit open time which gives a similar result, viz.  $4.2 \times 10^7 \text{ M}^{-1} \text{ s}^{-1}$ . Both of these estimates are valid for a simple blocker regardless of whether the activations produced by CCh contain (undetected) gaps of the type seen with other agonists in addition to blockages (see Ogden & Colquhoun, 1985, Appendix 2). The equilibrium constant for open-channel block by CCh is thus estimated as 1.8 mM at -130 mV. These estimates of the channel-blocking rates, derived from direct observations of putative blockages at low agonist concentrations, are similar to those found by Ogden & Colquhoun (1985) who used high CCh concentrations (up to 5 mM) and measured equilibrium block from the depression of the mean single-channel current, and block rates from the excess open-channel noise. They estimated the association rate as of  $7.3 \times 10^7 \text{ M}^{-1} \text{ s}^{-1}$ , the dissociation rate as  $11 \times 10^4 \text{ s}^{-1}$  (mean blockage length 9  $\mu\text{s}$ ), and the equilibrium constant as 1.5 mM.

*The intermediate gap component.* These gaps are unlikely to result from channel block by the agonist because their mean duration is very different from the independently determined mean length of blockages, for all the agonists tested here.

#### *Ion-channel block by other substances*

It is possible that gaps within bursts might be caused by block of the channel by agents other than the agonist, for example a muscle constituent or an ion in the bathing solution, or from some other ill-understood aspect of ion permeation. Such agents would produce blockages at a rate independent of agonist concentration, as observed. The lack of voltage dependence in the mean lifetime of gaps within bursts would suggest that dissociation rate of such a blocker was not voltage dependent (e.g. the blocker was uncharged). The number of gaps per unit open time, which would be interpreted as the association rate for a blocker, declined with hyperpolarization, as might be expected for a negatively charged agent working from the outside or a positively charged agent working from within the cell. The number of gaps per unit open time might be expected to be independent of the nature of the agonist for such a mechanism. In fact the rates were very similar for ACh and SubCh, but were rather lower for DecCh and possibly (see below) for CCh also. Such a mechanism cannot be ruled out conclusively.

*Effects of changing ion concentration.* The mean duration and frequency of short gaps

was found to be essentially unchanged by a 10-fold reduction in the extracellular concentration of either  $H^+$  or  $Ca^{2+}$ , so block by these ions is most unlikely. Furthermore there was little effect on either short or intermediate gaps when the internal  $[Cl^-]$  was raised, so block by  $Cl^-$  from inside is also unlikely. In one experiment it proved possible to make measurements with an isolated inside-out patch (with isotonic KCl on the cytoplasmic surface). Again the characteristics of short and intermediate gaps were unchanged, so block by any sort of diffusible intracellular molecule is unlikely to explain the interruptions that we observe; we cannot, of course, rule out the possibility that some blocking molecule might remain attached to the membrane even after the isolated patch formation.

An unexpected observation was made in the course of these experiments: reduction of the extracellular  $[Ca^{2+}]$  from 1.8 to 0.18 mM caused an approximately 10-fold increase in the mean number of intermediate gaps per long burst, and also a substantial increase in the single-channel conductance (from 30 to  $44 \pm 0.9$  pS). These effects were not seen when  $Ca^{2+}$  was replaced by  $Mg^{2+}$  so they appear to be effects of extracellular divalent cations. The following observations may be pertinent to these effects.

The effect of reduced  $[Ca^{2+}]$  on the end-plate channel conductance could be caused by a reduced screening of negative surface changes near the end-plate channel. This would cause an increase in the concentration of  $Na^+$  in the channel mouth (as compared to the concentration of  $Na^+$  in the bulk solution). Circumstantial evidence has been reported for the existence of negative surface changes at the end-plate (Cohen & Van der Kloot, 1978; Van der Kloot & Cohen, 1979; Lewis, 1979; Lewis & Stevens, 1979; Dreyer, Peper, Sterz, Bradley & Müller, 1979; Adams *et al.* 1980). The charge densities invoked range from 0.001 to 0.01  $e \text{ \AA}^{-2}$ . Calculations of the change in surface potential (e.g. Hille, Woodhull & Shapiro, 1975) when extracellular  $[Ca^{2+}]$  is reduced from 1.8 to 0.18 mM give 0.8 mV and 12.5 mV, respectively for the two charge densities above. The increased channel conductance can be accounted for only if the surface charge density is rather large (above 0.005  $e \text{ \AA}^{-2}$ ). Alternatively  $Ca^{2+}$  could modify the ion permeation mechanism by binding to a channel site.

The large effect of changing  $[Ca^{2+}]$  on the frequency of intermediate gaps cannot be accounted for at present. However, three sorts of interaction are to be expected: (a) occupancy of the presumably anionic binding site for ACh by divalent cations, (b) increase of the concentration of agonist close to the binding site, and (c) changes in the transmembrane voltage which affect voltage-dependent reactions. It has been shown that  $Ca^{2+}$  and  $Mg^{2+}$  inhibit a  $\alpha$ -bungarotoxin binding (presumably at the ligand-binding site) with apparent equilibrium dissociation constants in the range of 0.1–1 mM (Schmidt & Raftery, 1974).  $Ca^{2+}$  is released from the binding site upon ACh binding (Chang & Neumann, 1976; Neumann & Chang, 1976).

#### *Other possible explanations for gaps within bursts*

There are various other possibilities. For example, there might be short-lived shut states distal to the open states (e.g. short-lived desensitized states). Alternatively, the thermal fluctuations of the channel protein might be such that the channel was occasionally briefly occluded, or empty of ions. None of these possibilities is amenable to direct experimental test at present.

*The nature of the brief opening component*

The brief component in the distribution of apparent open times, or of burst lengths, was unsuspected from noise analysis but has been seen in several preparations, with a variety of agonists, by single-channel methods (Colquhoun & Sakmann, 1981; Cull-Candy & Parker, 1982; Jackson *et al.* 1982, 1983; Suarez-Isla, Wan, Lindstrom & Montal, 1983; Sine & Steinbach, 1984*a*, 1985; Takeda & Trautmann, 1984). However, in the only other study with ACh on junctional muscle receptors (of twitch fibres from the garter snake) a brief component was not seen (Dionne & Leibowitz, 1982; Leibowitz & Dionne, 1984). Again there are various possible mechanisms which will now be considered.

*Two sorts of channel*

There could be two independent types of channel, one producing mainly single brief openings, the other producing bursts of longer openings. This cannot be ruled out entirely. It is quite compatible with the observed correlation between open times and the observed concentration dependence of the relative number of short openings with SubCh could result from the two channels having different concentration-response curves, or different desensitization characteristics. On the other hand, the relative number of short openings was found to be reasonably reproducible from patch to patch. For this to occur there would have to be an even distribution of the two sorts of channel in the membrane, and a large number of channels in each patch. This is quite possible. However, the amplitude of the brief openings seemed to be similar to that of the long openings (though many of the brief openings were too short for their amplitude to be accurately measurable). Both have the amplitude expected for junctional type channels. The extrajunctional type of channel was seen very rarely in this work.

*Singly occupied channel openings*

It has been an obvious possibility, at least since the work of Karlin (1967), that channels might open with only one agonist molecule bound. If this were the origin of the 'short openings' then the ratio of the areas for the slow and fast components of the burst length distribution should increase approximately linearly with agonist concentration, even if there were two non-equivalent subunits (see simulation below). We observe such a linear relationship at low SubCh concentrations (Fig. 14), but at higher concentrations the relative number of 'short openings' does not fall as quickly as predicted. It could be that the rather small brief component (less than 15%) that remains at higher concentrations arises in some other way, though the fact that the time constant seems to be similar at high and low concentrations speaks against this.

Takeda & Trautmann (1984) also found that the relative number of brief openings was greater at low concentrations (for ACh on rat myotube cultures), and results very similar to ours have been made with purified reconstituted *Torpedo* receptor (M. Montal, personal communication).

On the other hand Sine & Steinbach (1984*a*, 1985) found with the BC3H-1 cell line that the relative number of short openings was independent of agonist concentration for ACh, CCh and dimethyltubocurarine (which is an agonist on these

cells). This is clearly inconsistent with the singly occupied explanation. Their observations also differ from ours in that they see far more short openings at high concentrations than we find here (e.g. 39 % for ACh, 10–500 nm). Clearly single occupation cannot explain either their short openings, or those seen at high agonist concentrations here; however, no specific suggestions have been made beyond postulation of some other open state related in an unknown way to those that produce the main (long) openings.

#### *Subconductance states*

Although subconductance states of the end-plate channel were observed regularly in our experiments, they were seen in only a very low (and rather variable) percentage of all elementary currents. Only about 0·4 % (range 0·1–0·8 %,  $n = 12$ ) of gaps within bursts were unambiguous partial closures, and about 1 % (range 0·2–3·2 %) of all long bursts contained partial closures.

Nicotinic receptor subconductance states have up to now been reported only for embryonic tissue in which the receptors have a fast metabolic turnover. The experiments reported here show that subconductance states occur regularly in the adult muscle fibre, which has metabolically stable receptors. The most interesting aspect of the subconductances states which we observe is that two discrete values are detectable, with mean amplitudes of 18 % and 71 % respectively of the main conductance state (Fig. 10). The less frequently observed 71 % state is comparable in its conductance with that reported for the non-synaptic channel in denervated frog muscle fibres (Neher & Sakmann, 1976). In fact we have very occasionally observed this lower-conductance channel in the end-plate region in isolation.

It seems likely that the channel (at least in *Torpedo*) is formed by five amphipathic helices, one from each subunit of the receptor-channel protein, (Guy, 1984) so it is easy to imagine barrel-like holes with several different open states.

The lower (18 %) conductance state of the end-plate channel is not observed in isolation and, because of its small conductance, it is more difficult to describe. It is similar in amplitude to the subconductance state observed in cultured chick muscle by Auerbach & Sachs (1983). The occurrence of this state presents a serious problem for the interpretation of short gaps, because the distinction between a complete closure and a partial closure to a subconductance state is not possible (with our data) for events shorter than 110  $\mu$ s. However, we think, for the reasons given above, that most of the brief gaps represent complete closures.

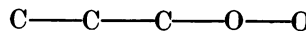
#### *Connexions between states*

It has been shown that correlations between open times can give information about the pathways that connect the various states in which the system can exist (Jackson *et al.* 1983; Fredkin, Montal & Rice, 1985; D. Colquhoun & A. G. Hawkes, in preparation).

The interpretation of correlations between burst lengths cannot be made quantitative with our data because the number of channels from which we are recording is unknown, so successive bursts may sometimes originate from different channels. This should not be a problem for interpretation of correlations between the first and second apparent opening within a burst, but the existence of undetected short gaps

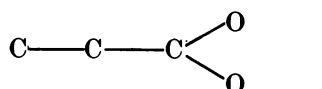
will interfere with this sort of measurement. Both problems affect measurements of correlations between apparent open times. These problems may be expected to reduce the size of any real correlation that may exist.

We have observed positive correlations between successive apparent open times, and between the first and second apparent open times within a burst, at the lowest SubCh concentrations. At higher concentrations correlations were not detectable (as might be expected from the rareness of short openings at higher concentrations). These observations suggest that there are at least two routes for transition between the open states and the gap-within-burst shut states (more strictly, that there is no *gateway* state between these subsets; see Fredkin *et al.* 1985; D. Colquhoun & A. G. Hawkes, *in preparation*). However, no correlations between successive burst lengths were detectable at any concentrations; this is consistent with there being only one route (more strictly, a gateway state) between the resting shut states and the burst states (open or shut). The former observations are inconsistent with schemes such as



or

(A)



in which C represents a closed state and O an open state.

This conclusion can also be reached by inspection of the distribution of the number of openings per burst. The mechanisms in scheme (A) have two open states so they predict that there will be two geometric components in this distribution (Colquhoun & Hawkes, 1982). However, for the particular cases in scheme (A) one of these components (that with unit mean) is predicted to have zero amplitude (J. H. Steinbach, personal communication; D. Colquhoun & A. G. Hawkes, *in preparation*). We, however, see very clearly two components, one with a near-unit mean (Fig. 17). Indeed this is much more obvious than are the rather small and erratic correlations. Therefore the mechanisms in scheme (A) are ruled out.

Similar conclusions concerning scheme (A) were reached by Jackson *et al.* (1983) who measured, essentially, an approximation to the correlation between the first and second apparent openings in a burst, with ACh in cultured rat muscle. Labarca, Rice, Fredkin & Montal (1985) recently reported correlations between apparent open times with reconstituted *Torpedo* receptor. It is difficult to compare either of these reports with ours because neither paper gives much detail concerning the distribution of shut times. The resolution in these experiments was 0.7 and 1 ms respectively, compared with 30–70  $\mu$ s here. If their data contained short gaps such as we see, they would have been missed entirely, so what they describe as openings would be what we describe as bursts; we can detect no correlations between burst lengths.

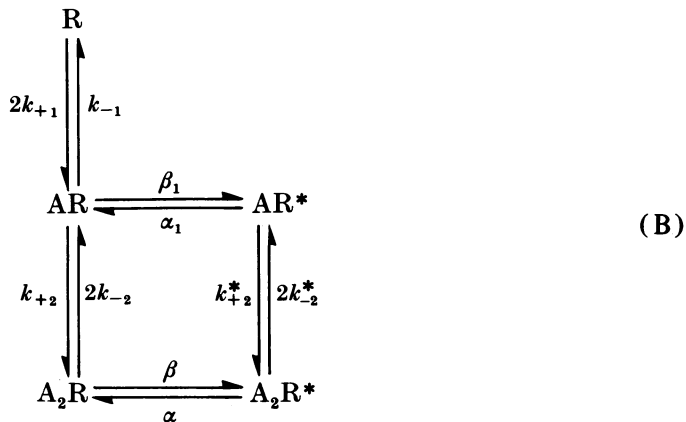
### Possible mechanisms

So far we have only described the observations, without commitment to any particular interpretation. Now we shall speculate about specific mechanisms. It must be said at the outset that the results are compatible with more than one mechanism, and that we cannot present any simple and physically plausible mechanism that will account for all of the observations.

It is certainly possible that the brief gaps within bursts result from sojourns in some unknown short-lived shut state, perhaps distal to the open state (the possible nature of such states was discussed above). Equally the component of brief openings could have various causes (see above) other than openings of singly occupied channels. If this were the case then single-channel measurements would not, at present, be interpretable in terms of mechanisms, so little could be learned that was not already known from noise analysis. Some of the results of Sine & Steinbach (1984a, 1985) favour this view; these are discussed below, but first we shall consider the extent to which less arbitrary schemes can account for the observations.

### Gaps as a result of multiple openings

The mechanism in scheme (B) originated in the extension by Karlin (1967) of the scheme of Castillo & Katz (1957), to account for the observed co-operativity in terms of the hypothesis of Monod, Wyman & Changeux (1965). It has been widely discussed since then (e.g. Colquhoun, 1973; Dreyer, Peper & Sterz, 1978; Dionne, Steinbach & Stevens, 1978; Colquhoun & Hawkes, 1982; Magleby & Pallotta, 1983). Letting R denote the shut receptor-channel molecule,  $R^*$  the open conformation, and A the agonist, we have



The transitions are labelled with their microscopic rate constants ( $k_{-1}$ ,  $k_{+1}$  etc.). There is no evidence that unoccupied channels can open in this preparation (cf. Jackson, 1984) so the  $R^*$  form has been omitted. In mechanisms such as scheme (B) interchange between the two open states is expected, on the basis of our data, to be very slow (see below) so omission of this pathway would make very little difference to our conclusions.

In this mechanism oscillations between  $A_2R^*$  and  $A_2R$  could cause short gaps

within bursts (longer gaps could result if AR were reached), and AR\* might represent brief openings.

*Inferences from brief gaps.* From scheme (B) we expected that the mean length of brief gaps within bursts (single sojourns in A<sub>2</sub>R) will be

$$\tau_f = 1/(\beta + 2k_{-2}) \quad (12)$$

and the mean number of such gaps per long burst will be

$$n_b = \beta/2k_{-2}. \quad (13)$$

Thus values for  $\beta$  and  $k_{-2}$  can be estimated for each agonist. The calculations are valid for any mechanism that involves AR ⇌ A<sub>2</sub>R ⇌ A<sub>2</sub>R\*. If the two binding sites were non-equivalent the value of  $k_{-2}$  given would represent the mean of the dissociation rates from the two sorts of site. The estimates, together with the corrected value of  $\alpha$  from Table 3, are given in Table 5 for ACh, SubCh and DecCh (CCh is considered below).

Strictly speaking, if intermediate gaps were to result essentially from sojourns in the singly occupied shut state (see below) then it can be shown that the definition of the burst used in eqns. (12) and (13) should exclude the intermediate gaps. The latter are however sufficiently rare that it makes little difference whether they are excluded or not.

*Predictions of potency.* The relative potency at equilibrium for scheme (B) should, for low concentrations, be proportional to  $[\beta/(\alpha K_1 K_2)]^{\frac{1}{2}}$  where  $K_1 = k_{-1}/k_{+1}$  and  $K_2 = k_{-2}/k_{+2}$  are the microscopic equilibrium constants for binding. A crude estimate of relative potency can be obtained from the results in Table 5 if we assumed that  $k_{+2}$ , and the ratio  $K_1/K_2$ , are the same for all agonists. Potency will then be proportional to

$$\frac{1}{k_{-2}} \left( \frac{\beta}{\alpha} \right)^{\frac{1}{2}}. \quad (14)$$

Values of this, relative to the value for ACh, are given in the last column of Table 5. SubCh and DecCh are predicted to be of similar potency, each being about three times as potent as ACh. This agrees reasonably with the finding that SubCh is 3·5–5 times as potent as ACh, and is equipotent with DecCh (Heeseman, 1981; D. C. Ogden and D. Colquhoun, unpublished).

*Voltage dependence of inferred rates.* Neither  $\tau_f$  nor  $n_b$  (see eqns. (12) and (13)) show much dependence on membrane potential, so the estimates of  $\beta$  and  $k_{-2}$  found from them show little voltage dependence. This is as expected. The fact that the equilibrium constant for binding of competitive antagonists (which presumably bind at the same site as the agonists) is not voltage dependent implies that the binding of agonists, and hence  $k_{-2}$ , is not likely to be voltage dependent (Colquhoun, Dreyer & Sheridan, 1979; Colquhoun & Sheridan, 1981). The evidence in the literature concerning the voltage dependence of  $\beta$  is more flimsy. Although it has been said that  $\beta$  is only slightly voltage dependent (e.g. Magleby & Stevens, 1972; Dionne & Stevens, 1975; Neher & Sakmann, 1975), on the grounds that the voltage dependence of the equilibrium response at low agonist concentration is similar to the voltage dependence of the mean channel lifetime, this result might reflect the voltage dependence of binding rather than that of the opening reaction (see below).

We have observed, in broad agreement with earlier work, that the directly observed frequency of channel activations (long bursts) is only slightly voltage dependent. A

hyperpolarization of  $350 \pm 90$  mV appeared to produce an e-fold increase in burst frequency, so over the potential range used in this work the burst frequency should change by no more than 30%.

TABLE 5. Estimates of rate constants that would be valid if short gaps within bursts represented multiple openings of the ion channel during a single occupancy (see text). The value of  $\alpha$  is taken from Table 3, and is that for a membrane potential of  $-130$  mV. The index of potency (see text) is the value relative to that for ACh

Agonist	$k_{-2}$ ( $s^{-1}$ )	$\beta$ ( $s^{-1}$ )	$\alpha$ ( $s^{-1}$ )	$\beta/\alpha$	Relative potency
ACh	8150 $\pm 600$	30600 $\pm 1180$	714	43	1
SubCh	2410 $\pm 180$	18000 $\pm 700$	625	29	2.8
DecCh	2420 $\pm 170$	9500 $\pm 300$	303	31	2.9

The interpretation of changes in the activation frequency is not as straightforward as has often been assumed. The frequency of individual openings can be written as  $f_o = p_o/m_o$ , and the burst frequency will be approximately  $f_b = p_o/m_b$ , where  $p_o$  is the probability (fraction of time) that a channel is open,  $m_o$  is the mean length of a single opening and  $m_b$  is the mean burst length (more exactly, the mean open time per burst).

For mechanisms such as scheme (B), if we ignore the possibility of singly occupied openings, then at sufficiently low concentrations we have

$$f_o \simeq \beta x_A^2 / K_1 K_2$$

and

$$f_b \simeq f_o / (1 + \beta / 2k_{-2}),$$

where  $x_A$  is the agonist concentration. Thus the opening frequency depends on  $\beta/K_1 K_2$ , so that effects of, for example, membrane potential on the channel opening rate and on binding cannot be distinguished. The same will be true for the burst frequency only for agonists that show few repeated openings ( $\beta \ll k_{-2}$ ), in which case  $f_o \simeq f_b$ .

If, at the other extreme, there were many repeated openings then the burst frequency would depend only on  $k_{+2}/K_1$ , so its voltage dependence would depend only on the voltage dependence of binding, and not at all on the voltage dependence of  $\beta$ . This is because, in this case, virtually every double occupancy would produce an opening, so that the exact value of  $\beta$  would be irrelevant. If  $\beta$  were in fact voltage dependent, but binding were not, the burst frequency would not be voltage dependent, but the opening frequency would be, because of voltage dependence in the mean number of openings per burst.

In summary, our evidence is consistent with both  $\beta$  and  $k_{-2}$  having a low voltage dependence, as found for the values in Table 5. The (marginally significant) tendency of short gaps to become shorter with hyperpolarization for SubCh showed an e-fold effect for 343 mV (see Fig. 5). This is of the order that might be expected from the voltage dependence of the burst frequency.

*Equilibrium constants for binding.* Even if short gaps can be interpreted in the manner described, the only information concerning binding is a single dissociation rate constant. If, however, we assume  $k_{-1} = k_{-2}$  and that  $K_1 = K_2$  (so  $k_{+1} = k_{+2}$ ) then the value of the equilibrium constant can be chosen to fit the known agonist potency at equilibrium.

For ACh, a good fit is obtained with  $K_1 = K_2 = 80 \mu M$ . In conjunction with

$k_{-2} = 8150 \text{ s}^{-1}$  (Table 5) this implies that  $k_{+1} = k_{+2} = 1.0 \times 10^8 \text{ M}^{-1} \text{ s}^{-1}$ , which is certainly a plausible value. Together with  $\beta/\alpha = 43$  (Table 5) these values imply that 50% of channels would be open (in the absence of desensitization) at an ACh concentration of  $14.4 \mu\text{M}$ , as is observed (Sakmann *et al.* 1980; Ogden, 1985). These values also imply that 50% of binding sites would be occupied at an ACh concentration of  $12 \mu\text{M}$  (in practice desensitization makes this virtually impossible to measure).

For SubCh and DecCh, if we assume that  $K_1 = K_2 = 15 \mu\text{M}$ ,  $k_{-1} = k_{-2} = 2410 \text{ s}^{-1}$  (Table 5) so  $k_{+1} = k_{+2} = 1.6 \times 10^8 \text{ M}^{-1} \text{ s}^{-1}$ , and  $\beta/\alpha = 29$  (Table 5), 50% of channels would be open at a concentration of  $3.4 \mu\text{M}$  (if it were not for channel block), so these agonists are about four times as potent as ACh, in accordance with observation. The predicted concentration for occupancy of 50% of binding sites is  $2.7 \mu\text{M}$ .

*Inferences about CCh.* Almost all the detectable short gaps with CCh are a result of channel block, so the above sort of analysis is impossible. Some speculations are, however, possible on the basis of the observed potency of CCh at equilibrium, viz. about 1/30th of the potency of ACh (Heeseman, 1981). This ratio, together with eqns. (12), (13) and (14) and the fact that the observed burst length of 1.3 ms is approximately given by  $(n_b + 1)/\alpha$ , suggests that  $\tau_f n_b \simeq 0.14 \mu\text{s}$  for CCh. We also know that CCh is capable of opening the channel for at least 80 or 90% of the time (Ogden & Colquhoun, 1983) so  $\beta/\alpha$  is unlikely to be less than about 8, which provides a limit for the values of the parameters (the first value in the inequalities given below). If we also assume that CCh is unlikely to be much *more* efficacious than ACh ( $\beta/\alpha < 80$ , say) we can obtain another limit (the second value in the inequality). The limits provided by these arguments are:  $0.03 < n_b < 0.1$ ;  $5 \mu\text{s} > \tau_f > 1.4 \mu\text{s}$ ;  $6000 \text{ s}^{-1} < \beta < 65000 \text{ s}^{-1}$ ;  $10^5 \text{ s}^{-1} < k_{-2} < 3 \times 10^5 \text{ s}^{-1}$ ; and, if we assume  $k_{+1} \simeq 10^8 \text{ M}^{-1} \text{ s}^{-1}$ , then  $1 \text{ mM} < K_2 < 3 \text{ mM}$ . The predicted mean number of gaps per burst is small so  $\alpha \simeq 1/1.3 \text{ ms} \simeq 770 \text{ s}^{-1}$ . The mean number of gaps per burst that would be detectable, with a resolution of say  $40 \mu\text{s}$ , is minute (less than  $10^{-5}$ ).

*Estimates of  $\beta$  by other methods.* The interpretation of short gaps in terms of multiple openings would be strengthened if the values of  $\beta$  so estimated agreed with estimates obtained by other methods. Unfortunately there are rather few good estimates.

Attempts to estimate  $\beta$  from noise and voltage-jump experiments with high agonist concentrations are technically difficult. They have been attempted by Sakmann & Adams (1979) and Adams (1981). With ACh it was not really possible to use high enough agonist concentrations to achieve clear saturation, so comparison with our results is not possible. Although saturation appeared clearer with CCh, it was achieved only at concentrations which are now known to produce channel block. The values of  $\beta$  of around  $2300 \text{ s}^{-1}$  for CCh so found may therefore be too small.

A completely different approach was used by Land, Salpeter & Salpeter (1981). They measured the rate of rise of miniature end-plate currents, after various amounts of  $\alpha$ -bungarotoxin block, at lizard intercostal muscle end-plates and concluded that  $\beta$  was about  $25000 \text{ s}^{-1}$  for ACh, a value which is close to that in Table 5. Furthermore, direct measurements of the fraction of time for which ACh can open the channel after elimination, as far as possible, of time spent in desensitized states suggest that  $\beta/\alpha$  is at least 30, again close to the value in Table 5 (Sakmann *et al.* 1980; Ogden & Colquhoun, 1983; Ogden, 1985).

Biochemical measurements based on ion-flux studies in electroplax vesicles have suggested that  $\beta/\alpha$  is only 0.67 for ACh (Cash, Aoshima & Hess, 1981), but this value is presumably measured near 0 mV. If only  $\alpha$  were voltage dependent and it was lengthened e-fold for, say, 70 mV hyperpolarization, then a value of  $\beta/\alpha = 43$  at -130 mV (Table 5) would correspond to  $\beta/\alpha = 6.7$  at 0 mV. This is still ten times larger than that found by Cash *et al.* (1981) possibly because of the twin problems of rapid desensitization and channel block by the large ACh concentrations used in this study.

**Efficacy and affinity.** From the point of view of structure-action relationships it is of interest to separate the contributions of binding (*affinity*), and of the events that follow binding (*efficacy*), to the over-all potency of agonists (Stephenson, 1956). In the present context  $K_1$  and  $K_2$  indicate affinity and  $\beta/\alpha$  measures efficacy (Castillo & Katz, 1957; Colquhoun, 1973). The values in Table 5 suggest that the least potent agonist, ACh, has the highest efficacy but the lowest affinity (the latter influence on potency being predominant). SubCh and DecCh probably have similar affinities, higher than that for ACh, but lower efficacies. Although the efficacy ( $\beta/\alpha$ ) is similar for SubCh and DecCh, both  $\beta$  and  $\alpha$  are faster, by a factor of about 2, for SubCh. DecCh produces only about half as many openings per burst but each opening is about twice as long. Efficacy, which is essentially an equilibrium concept, clearly provides an incomplete description, even in such a simple case as this.

**The rate-limiting step.** The (admittedly speculative) values given in Table 5 are inconsistent with the hypothesis of Anderson & Stevens (1973) that binding is very fast compared with conformation change (these authors made it clear that there was no real evidence, one way or the other, at that time). This hypothesis implies that openings will usually occur singly, which is not the case (except, probably, for CCh). It also implies that most bindings will dissociate straight away without ever producing an opening, which would lead to rather inefficient synaptic transmission if it were true for ACh. Fast binding could probably not compensate for this because of the diffusion limit on the association rate.

**Synaptic efficiency.** The values suggested for ACh in Table 5 would make it a near-ideal fast transmitter (Colquhoun & Sakmann, 1983), having a fast opening rate and low affinity so that it can dissociate rapidly. Rather similar values have been shown to account for the rise time of miniature end-plate currents in lizard muscle (Land *et al.* 1981). The numerical simulations of the miniature end-plate current done by Madsen, Edeson, Lam & Milne (1984), with rate constants not greatly different from those in Table 5, also suggest that these values are entirely consistent with the time course of physiological events.

#### *A detailed simulation for SubCh*

The values suggested above will now be used to make detailed predictions for SubCh on the basis of scheme (B). The values are  $k_{+1} = k_{+2} = 1.6 \times 10^8 \text{ M}^{-1} \text{ s}^{-1}$ ,  $k_{-1} = k_{-2} = 2410 \text{ s}^{-1}$ ,  $\beta = 18000 \text{ s}^{-1}$ ,  $\alpha = 625 \text{ s}^{-1}$ . Scheme (B) also includes the hypothesis that singly occupied channels can open (though this can be omitted without greatly affecting the other predictions). On the basis of the time constant of the brief openings (0.16 ms) we take  $\alpha_1 = 6250 \text{ s}^{-1}$ . A value for the opening rate  $\beta_1$ , for singly liganded channels can be obtained as follows. It was pointed out in the Results that

the plot against agonist concentration of the ratio of the number of long bursts to the number of short bursts had a slope (at low concentrations) of  $1.7 \times 10^8 \text{ M}^{-1}$ . There is not likely to be much direct interchange between the two open states, so this slope should be given approximately by

$$\frac{\beta}{\beta_1 2K_2 (1 + \beta/2k_{-2})}. \quad (15)$$

TABLE 6. Predicted characteristics of SubCh at 4 nM and 100 nM

Model	SubCh (4 nM)		SubCh (100 nM)	
No. of openings per burst	1 (59 %)	4.7 (41 %)	1.0003 (5.3 %)	4.8 (94.7 %)
Burst length	1 (59 %)	0.16 ms (41 %)	0.16 ms (5.4 %)	7.8 ms (94.6 %)
Length of gaps within bursts	1 (99.96 %)	43.8 $\mu$ s (0.04 %)	43.8 $\mu$ s (99.8 %)	0.41 ms (0.2 %)
	2 (99.7 %)	43.8 $\mu$ s (0.3 %)	43.8 $\mu$ s (98.5 %)	1.2 ms (1.5 %)
	3 (99.6 %)	43.8 $\mu$ s (0.4 %)	43.8 $\mu$ s (98.6 %)	1.3 ms (1.4 %)
Mean no. of gaps within burst per unit open time	1	0.48 ms <sup>-1</sup>	0.49 ms <sup>-1</sup>	
Correlations				
$r_1$ (openings)	1	0.073	0.004	
$r_2$ (bursts)	1	0.0004	0.00002	
	2	0.004	0.0002	
$r_{12}$ (bursts)	1	0.002	0.00008	
	2	0.02	0.0007	

Model 1 is scheme (B) with  $K_1 = K_2$ . Model 2 is scheme (B) with  $K_1 \neq K_2$ . Model 3 is scheme (C). The values used for the rate constants are given in the text. The areas for two-component distributions are given in parentheses. The distributions of the number of openings per burst, and of the burst length, are very similar for all three models so only one set of values is given. The burst length distribution has got four components in principle; the areas of the two that have been omitted are less than 0.04 %. The autocorrelation coefficients given are defined thus:  $r_1$  = correlation between open times with lag = 1;  $r_2$  = correlation between the first and second open time in bursts with two or more openings;  $r_{12}$  as  $r_2$ , but for bursts with exactly two openings only. The values of  $r_1$  are similar for all three models, and the values of  $r_2$  and  $r_{12}$  are similar for models 2 and 3.

This result can be found as the relative opening rates from  $A_2R$  and from  $AR$  (i.e. their occupancy multiplied by the opening rate constant), corrected for the mean number of openings per burst. It is also given by the relative probability that a burst starts in  $A_2R^*$  or  $AR^*$  (Colquhoun & Hawkes, 1982).

Substitution of the values above into eqn. (15) gives  $\beta_1 = 0.72 \text{ s}^{-1}$ . Microscopic reversibility implies that the affinity for the open form is very high,  $K_2^* = 0.06 \text{ nM}$ . If we assumed that the association rate constant for binding to the open form,  $k_{+2}^*$ , is the same as the others, then the dissociation rate constant from the open form would be very slow, viz.  $k_{-2}^* = 0.0096 \text{ s}^{-1}$ . These rates predict that 50 % of channels will be open at  $3.5 \mu\text{M}$ , and the Hill slope at this point will be 1.63.

The behaviour of the system can now be calculated as described by Colquhoun & Hawkes (1982, and in preparation). These calculations are for a single channel, but they are valid for a patch with many channels as long as activations are rare (as in this work) and no attempt is made to interpret quantitatively the shut times between activations.

*Agreement with observations.* The results are shown in Table 6 (model 1). In most respects there is close agreement with the experimental results. There are, however, two main respects in which the calculations do not make correct predictions (these are considered further below). (a) The number of long bursts relative to the number of short bursts increases linearly with concentration (line with unit slope in Fig. 14), whereas at concentrations above 20 nM the observations show rather more short openings than is predicted. (b) The observed time constant (1.2 ms, Table 1) of the intermediate component of the distribution of the length of gaps within bursts is longer than, though of the same order as, the calculated value (0.4 ms  $\approx 1/k_{-1}$ , which is approximately the mean length of a single sojourn in AR), but the calculated area (0.2% at 100 nM) is smaller than was observed (2.9%).

The predicted correlations between open times become negligible at higher concentrations, as observed. The scheme (B) predicts that correlations between burst lengths will be zero, because all bursts must start from the one resting state, R (D. Colquhoun & A. G. Hawkes, in preparation), which is consistent with the observations. The calculations also predict that the mean lengths of openings and gaps will be very similar, regardless of their position within the burst, for all bursts with two or more openings (much as in the similar example given by Colquhoun & Hawkes, 1982). Short openings will be rare in such bursts. Again these predictions agree with the experiments.

The noise spectrum calculated for this example (100 nM-SubCh) consists almost entirely of a single Lorentzian spectrum with a time constant of 7.8 ms (virtually the same as that for the slow component of the burst length distribution). The largest of the other three components has a zero-frequency amplitude that is almost four orders of magnitude smaller than the 7.8 ms component.

*Could  $\beta$  be larger?* It is possible to fit the observed burst length and equilibrium potency in other ways. For example, if we continue to assume that  $K_1 = K_2$  then it is possible to fit them with the affinity, and  $\beta/\alpha$ , having much the same values as above, but with both  $\beta$  and  $\alpha$  being much larger. A burst would therefore be made up of a large number of very short openings separated by very short (undetectable) gaps. If  $K_1$  and  $K_2$  are not assumed to be the same then the burst length and potency can be fitted with  $K_1$  considerably less than  $K_2$  (negative co-operativity in binding),  $\beta$  larger, but  $\alpha$  as above, so the number of openings per burst would be much as above the gaps within bursts would be very short and therefore undetectable.

In both of these cases it would be necessary to find some other explanation for the observed brief gaps (some possibilities were discussed earlier). Furthermore, in both cases (particularly the former) the results would be incompatible with the fast-binding hypothesis (Anderson & Stevens, 1973).

*Intermediate gaps as a result of multiple openings?* It might be suggested that the small intermediate component of gaps within bursts, rather than the brief component, represent sojourns in the shut state that immediately precede opening. If this were

the case then the argument used above would give, for example,  $\beta/\alpha = 0.46$  for ACh, so this agonist would be capable of opening only about 30% of channels. This is contrary to observation (Sakmann *et al.* 1980; Ogden & Colquhoun, 1983; Ogden, 1985).

*Unequal binding constants.* So far it has been assumed that  $K_1 = K_2$  in scheme (B). If this assumption is relaxed, the only improvement in the fit to the results presented here concerns the intermediate gap component. The reason for the very small predicted area for this component (Table 6, model 1) is that once AR is reached the next transition is almost certain to be to R (at low agonist concentrations), rather than back via A<sub>2</sub>R to the open state. But only in the latter case is an intermediate gap produced. This effect would be less pronounced if  $k_{+2}$  were increased, and  $k_{-1}$  decreased. The latter change would also increase the mean length of intermediate gaps to a value closer to that observed (1.2 ms). The observed short gap frequency dictates that  $k_{-2}$  must not be changed, but  $k_{+1}$  can be reduced to achieve the correct equilibrium potency.

It can be shown, by the cluster analysis of Colquhoun & Hawkes (1982), that the relative area of the intermediate gap component should increase linearly with concentration, at low concentrations, as long as singly occupied channels cannot open. If they can open, the increase will be less than linear at very low concentrations.

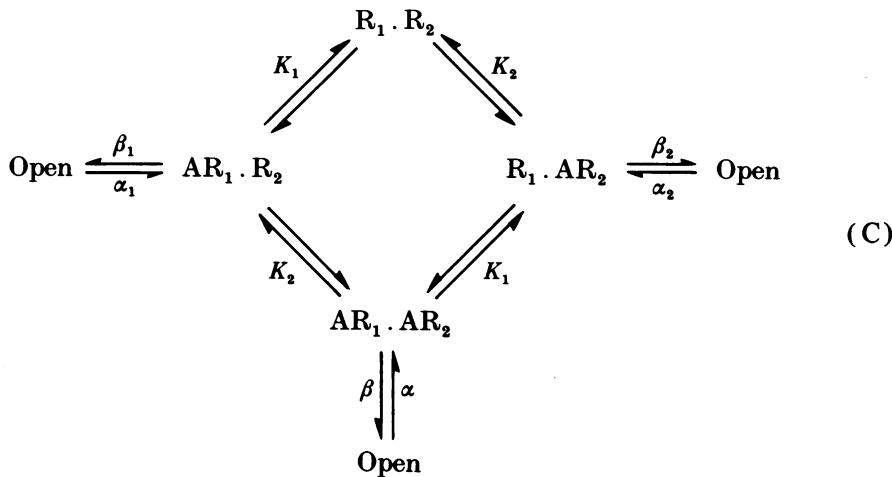
The values in Table 5 (model 2) were calculated for  $\alpha = 625 \text{ s}^{-1}$ ,  $\beta = 18000 \text{ s}^{-1}$ ,  $\alpha_1 = 6520 \text{ s}^{-1}$  (all as before), with  $\beta_1 = 2.3 \text{ s}^{-1}$ ,  $k_{+1} = 1.2 \times 10^7 \text{ M}^{-1} \text{ s}^{-1}$ ,  $k_{-1} = 800 \text{ s}^{-1}$ ,  $k_{+2} = 5 \times 10^8 \text{ M}^{-1} \text{ s}^{-1}$  and  $k_{-2} = 2410 \text{ s}^{-1}$ . The values of  $K_1$  (67  $\mu\text{M}$ ) and  $K_2$  (4.8  $\mu\text{M}$ ) imply some inherent positive co-operativity in binding in this case. These rates predict that 50% of channels will be open at 3.6  $\mu\text{M}$ -SubCh; the Hill slope at this point will be 1.90 (steeper than when  $K_1 = K_2$ ).

It can be seen that both the time constant and the relative area for the intermediate gap component are closer to the observed values than before. There is some suggestion in the data (see Results) that the area of this component increases with concentration as predicted, but the scatter is such that a precise comparison cannot be made. The predicted correlations within bursts are ten times larger than before (but still very small).

#### *Non-equivalent subunits*

There is a substantial amount of biochemical evidence that the two  $\alpha$  subunits of the nicotinic receptor are not equivalent, at least in the receptor from *Torpedo* and the BC3H-1 cell line (see, for example, Sine & Taylor, 1981). If we assume, for simplicity, that the rate constant for binding to one subunit is independent of whether or not a molecule is bound to the other subunit (i.e. no inherent co-operativity in binding) then we have scheme (C) (see over). Here R<sub>1</sub> and R<sub>2</sub> represent the two sorts of subunits with equilibrium binding constants  $K_1 = k_{-1}/k_{+1}$  and  $K_2 = k_{-2}/k_{+2}$  respectively.

The predictions are very similar to those just found for scheme (B) with  $K_1 \neq K_2$ , the improvement over the basic model being restricted to the intermediate gap component. The values in Table 6 (model 3) were found from scheme (C) with rate constants as follows:  $\alpha = 625 \text{ s}^{-1}$ ;  $\beta = 18000 \text{ s}^{-1}$ ;  $\alpha_2 = 6250 \text{ s}^{-1}$  (all as before); with  $\beta_1 = 0$ ,  $\beta_2 = 2.7 \text{ s}^{-1}$ ;  $k_{+1} = 5 \times 10^8 \text{ M}^{-1} \text{ s}^{-1}$ ;  $k_{-1} = 4070 \text{ s}^{-1}$ ;  $k_{+2} = 2.8 \times 10^7 \text{ M}^{-1} \text{ s}^{-1}$ , and  $k_{-2} = 750 \text{ s}^{-1}$ . The numbering of the subunits is, of course, arbitrary, so the



different values of  $K_1$  ( $8.1 \mu\text{M}$ ) and  $K_2$  ( $26.8 \mu\text{M}$ ) represent the heterogeneity of the subunits rather than co-operativity in binding. The values predict that 50% of channels will be open at  $3.5 \mu\text{M}$ -SubCh, and that the Hill slope at this point will be 1.64 (like model 1, but shallower than model 2).

#### *Comparison with other short-gap measurements*

Many workers have now observed brief shut periods during a single activation, in various agonist-activated channels (Colquhoun & Sakmann, 1981, 1983; Cull-Candy & Parker, 1982; Dionne & Leibowitz, 1982; Auerbach & Sachs, 1983, 1984; Leibowitz & Dionne, 1984; Sine & Steinbach, 1984*a*, 1985).

Leibowitz & Dionne (1984) observed short gaps with a mean duration of about  $200 \mu\text{s}$ , and about 0.2 gaps per burst (though they did not use a burst analysis) for ACh on garter snake twitch fibres at  $-100 \text{ mV}$ . Their gaps are 10 times longer, and much rarer, than those we find with ACh; also, unlike ours, they become much briefer on hyperpolarization. They, like us, were unable to resolve short gaps with CCh. If their results were interpreted according to the multiple-opening hypothesis, they found, for ACh at  $-100 \text{ mV}$ ,  $\beta \approx 800 \text{ s}^{-1}$  and  $k_{-2} \approx 2000 \text{ s}^{-1}$  (in our notation; their  $k_{-2}$  is the macroscopic rate constant). Unlike our values, these are strongly voltage dependent, both getting faster with hyperpolarization. These values (especially  $\beta$ ) are smaller than ours, and  $\beta$  seems rather small to account for the rapid rise of the miniature end-plate current. However, there are no independent estimates of  $\beta$  on this preparation so there is no way of checking whether the interpretation is correct.

Sine & Steinbach (1984*a*, 1986) found, on the BC3H-1 cell line, short gaps of mean duration  $50-60 \mu\text{s}$  for ACh, CCh, SubCh and also for dimethyltubocurarine (DMT) which is an agonist on these cells. These values are much less dependent on the nature of the agonist than ours. We detected no short gaps with CCh (as might be expected for an agonist with low affinity), whereas they found 1.3 per burst, almost as many as with ACh and SubCh. There are thus substantial differences between our observations and theirs. Nevertheless, the values of  $\beta$  and  $k_{-2}$  that they infer from the multiple-opening hypothesis are not implausible for ACh and SubCh, though

again there is no independent estimate of either on this preparation, with which to compare the values. Their most interesting observation, however, is that gaps of very similar length to those with ACh (though rather rarer, 0·6 per burst) were found with DMT. This, if interpreted according to the multiple-opening hypothesis, would suggest a value of  $6000\text{ s}^{-1}$  for  $\beta$  which is quite unreasonably high for what must be assumed to be a weak agonist. They therefore conclude, very reasonably, that the short gaps cannot be interpreted according to the multiple opening hypothesis, and that the gaps probably represent a separate, fully occupied shut state distal to the open state. An agonist of low efficacy and high affinity, such as DMT is supposed to be, should indeed provide a good test of the multiple-opening hypothesis. DMT may, however, be less than ideal for this purpose, (a) because of its very powerful channel-blocking action (equilibrium constant probably less than 50 nM, i.e. 1/60th of the lowest concentration used), and (b) because, although it is helpful that binding experiments have been done with DMT (Sine & Taylor, 1981), the fact that it was subsequently found to be an agonist must inevitably complicate the interpretation of these experiments.

#### *Conclusions concerning mechanisms*

The component of brief openings behaves at low concentrations as though it originated from openings of singly occupied channels. However, the persistence of about 10% of apparently similar brief openings at higher concentrations is incompatible with this view, so it is unlikely that *all* brief openings have this mechanism.

The short gaps within bursts behave, in our preparation, in a way that is consistent with the view that they originate from multiple openings of the doubly occupied channel, before dissociation occurs. The evidence for this mechanism is circumstantial, and the results are consistent with other mechanisms. However, the values for the opening and dissociation rate so found are consistent with the relative potencies of the agonists, the results of high concentration experiments, and, in the case of ACh, the phenomena of synaptic transmission.

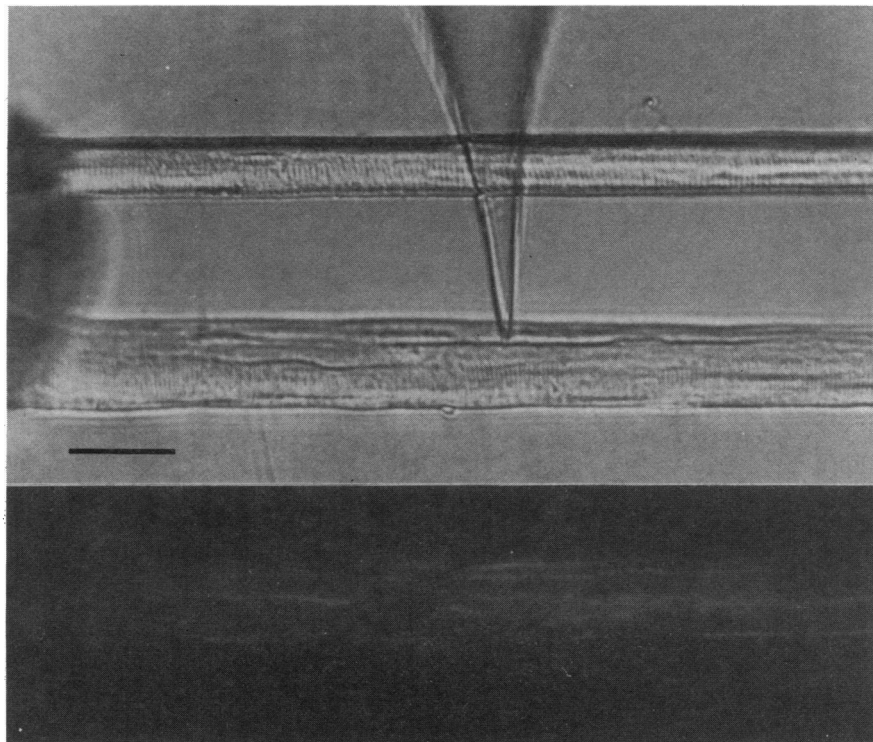
This work was supported by the M.R.C., and by a twinning grant from the European Science Foundation. We are grateful for discussions with Dr J. H. Steinbach, Professor A. G. Hawkes and Dr V. E. Dionne, and we thank Dr J. Heeseman for giving us various agonists.

#### REFERENCES

- ADAMS, D. J., DWYER, T. M. & HILLE, B. (1980). The permeability of end-plate channels to monovalent and divalent metal cations. *Journal of General Physiology* **75**, 493–510.
- ADAMS, P. R. (1981). Acetylcholine receptor kinetics. *Journal of Membrane Biology* **58**, 161–174.
- ANDERSON, C. R. & STEVENS, C. F. (1973). Voltage clamp analysis of acetylcholine produced end-plate current fluctuations at frog neuromuscular junction. *Journal of Physiology* **235**, 655–691.
- AUERBACH, A. & SACHS, F. (1983). Flickering of a nicotinic ion channel to a subconductance state. *Biophysical Journal* **42**, 1–10.
- AUERBACH, A. & SACHS, F. (1984). Single-channel currents from acetylcholine receptors in embryonic chick muscle. *Biophysical Journal* **45** 187–198.
- BOYLE, P. J. & CONWAY, E. J. (1941). Potassium accumulation in muscle and associated changes. *Journal of Physiology* **100**, 1–63.

- BREGESTOWSKI, P. D., MILEDI, R. & PARKER, I. (1979). Calcium conductance of acetylcholine induced end-plate channels. *Nature* **279**, 638–639.
- CASH, D. J., AOSHIMA, H. & HESS, G. P. (1981). Acetylcholine-induced cation translocation across cell membranes and inactivation of the acetylcholine receptor: chemical kinetic measurement in the millisecond time region. *Proceedings of the National Academy of Sciences of the U.S.A.* **78**, 3318–3322.
- CASTILLO, J. DEL & KATZ, B. (1957). Interaction at end-plate receptors between different choline derivatives. *Proceedings of the Royal Society B* **146**, 369–381.
- CHANG, W. & NEUMANN, E. (1976). Dynamic properties of isolated acetylcholine receptor proteins. Release of calcium ions caused by acetylcholine binding. *Proceedings of the National Academy of Sciences of the U.S.A.* **73**, 3364–3368.
- CLAPHAM, D. E. & NEHER, E. (1984). Substance P reduces acetylcholine-induced currents in isolated bovine chromaffin cells. *Journal of Physiology* **347**, 255–277.
- COHEN, I. & VAN DER KLOOT, W. G. (1978). Effects of  $\text{Ca}^{2+}$  and  $\text{Mg}^{2+}$  on the decay of miniature end-plate currents. *Nature* **271**, 77–79.
- COLQUHOUN, D. (1973). The relation between classical and cooperative models for drug action. *Drug Receptors*, ed. RANG, H. P., pp. 149–182. London: Macmillan.
- COLQUHOUN, D., DREYER, F. & SHERIDAN, R. E. (1979). The actions of tubocurarine at the frog neuromuscular junction. *Journal of Physiology* **293**, 247–284.
- COLQUHOUN, D. & HAWKES, A. G. (1977). Relaxation and fluctuations of membrane current that flow through drug-operated ion channels. *Proceedings of the Royal Society B* **199**, 231–262.
- COLQUHOUN, D. & HAWKES, A. G. (1981). On the stochastic properties of single ion channels. *Proceedings of the Royal Society B* **211**, 205–235.
- COLQUHOUN, D. & HAWKES, A. G. (1982). On the stochastic properties of bursts of single ion channel openings and of clusters of bursts. *Philosophical Transactions of the Royal Society B* **300**, 1–59.
- COLQUHOUN, D. & HAWKES, A. G. (1983). The principles of the stochastic interpretation of ion channel mechanisms. In *Single Channel Recording*, ed. SAKMANN, B. & NEHER, E. New York: Plenum Press.
- COLQUHOUN, D. & SAKMANN, B. (1981). Fluctuations in the microsecond time range of the current through single acetylcholine receptor ion channels. *Nature* **294**, 464–466.
- COLQUHOUN, D. & SAKMANN, B. (1983). Bursts of openings in transmitter-activated ion channels. In *Single Channel Recording*, ed SAKMANN, B. & NEHER, E. New York: Plenum Press.
- COLQUHOUN, D. & SHERIDAN, R. E. (1981). The modes of action of gallamine. *Proceedings of the Royal Society B* **211**, 181–203.
- COLQUHOUN, D. & SIGWORTH, F. J. (1983). Fitting and statistical analysis of single channel records. In *Single Channel Recording*, ed. SAKMANN, B. & NEHER, E. New York: Plenum Press.
- CULL-CANDY, S. G. & PARKER, I. (1982). Rapid kinetics of single glutamate-receptor channels. *Nature* **295**, 410–412.
- DAVID, F. N. & BARTON, D. E. (1962). *Combinatorial Chance*. London: Charles Griffin.
- DIIONNE, V. E. & LEIBOWITZ, M. (1982). Acetylcholine receptor kinetics: a description from single-channel currents at snake neuromuscular junctions. *Biophysical Journal* **39**, 253–261.
- DIIONNE, V. E., STEINBACH, J. H. & STEVENS, C. F. (1978). An analysis of the dose-response relationship at voltage-clamped frog neuromuscular junctions. *Journal of Physiology* **281**, 421–444.
- DIIONNE, V. E. & STEVENS, C. F. (1975). Voltage dependence of agonist effectiveness at the frog neuromuscular junction: resolution of a paradox. *Journal of Physiology* **251**, 245–270.
- DREYER, F., PEPPER, K. & STERZ, R. (1978). Determination of dose-response curves by quantitative ionophoresis at the frog neuromuscular junction. *Journal of Physiology* **281**, 395–419.
- DREYER, F., PEPPER, K., STERZ, R., BRADLEY, R. J. & MÜLLER, K. D. (1979). Drug receptor interaction at the frog neuromuscular junction. *Progress in Brain Research* **49**, 212–223.
- FREDKIN, D. R., MONTAL, M. & RICE, J. A. (1985). Identification of aggregated Markovian models: application to the nicotinic acetylcholine receptor. In *Proceedings of the Berkeley Conference in Honor of Jerzy Neyman and Jack Kiefer*. Belmont, CA: Wadsworth Publishing Co. (in the Press).
- GARDNER, P., OGDEN, D. C. & COLQUHOUN, D. (1984). Conductances of single ion channels opened by nicotinic agonists are indistinguishable. *Nature* **309**, 160–162.
- GOLDBERG, G. & LASS, Y. (1983). Evidence for acetylcholine receptor blockade by intracellular hydrogen ions in cultured chick myoballs. *Journal of Physiology* **343**, 429–437.

- GUY, H. R. (1984). A structural model of the acetylcholine receptor channel based on partition energy and helix packing. *Biophysical Journal* **44**, 249–261.
- HAMIL, O. P., MARTY, A., NEHER, E., SAKMANN, B. & SIGWORTH, F.J. (1981). Improved patch-clamp techniques for high-resolution current recording from cells and cell-free membrane patches. *Plügers Archiv* **391**, 85–100.
- HAMIL, O. P. & SAKMANN, B. (1981). Multiple conductance states of single acetylcholine receptor channels in embryonic muscle cells. *Nature* **294**, 462–464.
- HAMMES, G. G. (1979). Temperature jump methods. In *Techniques of Chemistry*, ed. HAMMES, G. G., vol. VI B, **343**, New York: Wiley-Interscience.
- HEESEMAN, J. (1981). Vergleichende elektrophysiologische Untersuchungen von synthetischen quarternären  $\alpha,\omega$ -Diammoniumverbindungen an der Froschmuskelendplatte. Inaugural Dissertation, Fachbereiche Medizin der Georg-August-Universität zu Göttingen.
- HILLE, B., WOODHULL, A. M. & SHAPIRO, B. I. (1975). Negative surface charge near sodium channels of nerve: divalent ions, monovalent ions, and pH. *Philosophical Transactions of the Royal Society B* **270**, 301–318.
- JACKSON, M. B. (1984). Spontaneous openings of the acetylcholine receptor channel. *Proceedings of the National Academy of Sciences of the U.S.A.* **81**, 3901–3904.
- JACKSON, M. B., LECAR, H., ASKANAS, V. & ENGEL, W. K. (1982). Single cholinergic receptor channel currents in cultured human muscle. *Journal of Neuroscience* **2**, 1465–1473.
- JACKSON, M. B., WONG, B. S., MORRIS, C. E., LECAR, H. & CHRISTIAN, C. N. (1983). Successive openings of the same acetylcholine receptor channel are correlated in open time. *Biophysical Journal* **42**, 109–114.
- KARLIN, A. (1967). On the application of 'a plausible model' of allosteric proteins to the receptor for acetylcholine. *Journal of Theoretical Biology* **16**, 306–320.
- KARLIN, A., COX, R., KALDANY, R.-R., LOBEL, P. & HOLTZMAN, E. (1983). The arrangement and functions of the chains of the acetylcholine receptor of *Torpedo* electric tissue. *Cold Spring Harbor Symposia on Quantitative Biology* **48**, 1–8.
- KATZ, B. & MILEDI, R. (1972). The statistical nature of the acetylcholine potential and its molecular components. *Journal of Physiology* **224**, 665–699.
- LABARCA, P., RICE, J. A., FREDKIN, D. R. & MONTAL, M. (1985). Kinetic analysis of channel gating: application to the cholinergic receptor channel and the chloride channel from *Torpedo californica*. *Biophysical Journal* **47**, 469–478.
- LAND, B. R., SALPETER, E. E. & SALPETER, M. M. (1981). Kinetic parameters for acetylcholine interaction in intact neuromuscular junction. *Proceedings of the National Academy of Sciences of the U.S.A.* **78**, 7200–7204.
- LANDAU, E. M., GAVISH, B., NACHSHEN, D. A. & LOTAN, I. (1981). pH dependence of the acetylcholine receptor channel: a species variation. *Journal of General Physiology* **77**, 647–666.
- LÄUGER, P. (1983). Conformational transitions of ionic channels. In *Single Channel Recording*, ed SAKMANN, B. & NEHER, E. New York: Plenum Press.
- LEIBOWITZ, M. D. & DIONNE, V. E. (1984). Single-channel acetylcholine receptor kinetics. *Biophysical Journal* **45**, 153–163.
- LEWIS, C. A. (1979). Ion concentration dependence of the reversal potential and the single channel conductance of ion channels at the frog neuromuscular junction. *Journal of Physiology* **286**, 417–445.
- LEWIS, C. A. & STEVENS, C. F. (1979). Mechanism of ion permeation through channels in a postsynaptic membrane. In *Membrane Transport Processes* **3**, ed. STEVENS, C. F. & TSIEN, R. W., pp. 89–103. New York: Raven Press.
- MADSEN, B. W., EDESON, R. O., LAM, H. S. & MILNE, R. K. (1984). Numerical simulation of miniature endplate currents. *Neuroscience Letters* **48**, 67–74.
- MAGLEBY, K. L. & PALLOTTA, B. S. (1983). Burst kinetics of single calcium-activated potassium channels in cultured rat muscle. *Journal of Physiology* **344**, 605–623.
- MAGLEBY, K. L. & STEVENS, C. F. (1972). A quantitative description of end-plate currents. *Journal of Physiology* **223**, 173–197.
- MARTY, A. (1980). Action of calcium ions on acetylcholine sensitive channels in *Aplysia* neurones. *Journal de physiologie* **76**, 523–527.
- MONOD, J., WYMAN, J. & CHANGEUX, J. P. (1965). On the nature of allosteric transitions: a plausible model. *Journal of Molecular Biology* **12**, 88–118.



- NEHER, E. & SAKMANN, B. (1975). Voltage-dependence of drug-induced conductance in frog neuromuscular junction. *Proceedings of the National Academy of Sciences of the U.S.A.* **72**, 2140–2144.
- NEHER, E. & SAKMANN, B. (1976). Noise analysis of drug induced voltage clamp currents in denervated frog muscle fibres. *Journal of Physiology* **258**, 705–729.
- NEUMANN, E. & CHANG, W. (1976). Dynamic properties of isolated acetylcholine receptor protein. Kinetics of the binding of acetylcholine and Ca ions. *Proceedings of the National Academy of Sciences of the U.S.A.* **73**, 3994–3998.
- OGDEN, D. C. (1985). The dependence of channel opening probability on acetylcholine concentration at the frog neuromuscular junction. *Journal of Physiology* **365**, 77P.
- OGDEN, D. C. & COLQUHOUN, D. (1983). The efficacy of agonists at the frog neuromuscular junction studied with single channel recording. *Pflügers Archiv* **399**, 246–248.
- OGDEN, D. C. & COLQUHOUN, D. (1985). Ion channel block by acetylcholine, carbachol and suberyldicholine at the frog neuromuscular junction. *Proceedings of the Royal Society B* (in the Press).
- SAKMANN, B. & ADAMS, P. R. (1979). Biophysical aspects of agonist action at frog endplate. In *Advances in Pharmacology and Therapeutics*, vol. 1, *Receptors*, ed. JACOB, J., pp. 81–90. Oxford: Pergamon Press.
- SAKMANN, B. & NEHER, E. (1983). Geometric parameters of pipettes and membrane patches. In *Single Channel Recording*, ed. SAKMANN, B. & NEHER, E. New York: Plenum Press.
- SAKMANN, B., PATLAK, J. & NEHER, E. (1980). Single acetylcholine-activated channels show burst-kinetics in presence of desensitizing concentrations of agonist. *Nature* **286**, 71–73.
- SCHMIDT, J. & RAFTERY, M. A. (1974). The cation sensitivity of the acetylcholine receptor from *Torpedo californica*. *Journal of Neurochemistry* **23**, 617–623.
- SCUKA, M. (1977). The effect of pH on the conductance change evoked by iontophoresis at the frog neuromuscular junction. *Pflügers Archiv* **369**, 239–244.
- SINE, S. M. & STEINBACH, J. H. (1984a). Activation of a nicotinic acetylcholine receptor. *Biophysical Journal* **45**, 175–185.
- SINE, S. M. & STEINBACH, J. H. (1984b). Agonists block currents through acetylcholine receptor channels. *Biophysical Journal* **46**, 277–283.
- SINE, S. M. & STEINBACH, J. H. (1986). Acetylcholine receptor activation by a site-selective ligand: nature of brief open and closed states in BC3H-1 cells. *Journal of Physiology* (in the Press).
- SINE, S. M. & TAYLOR, P. (1981). Relationship between reversible antagonist occupancy and the functional capacity of the acetylcholine receptor. *Journal of Biological Chemistry* **256**, 6692–6699.
- STEPHENSON, R. P. (1956). A modification of receptor theory. *British Journal of Pharmacology* **11**, 379–393.
- SUAREZ-ISLA, B. A., WAN, K., LINDSTROM, J. & MONTAL, M. (1983). Single-channel recordings from purified acetylcholine receptors reconstituted in bilayers formed at the tip of patch pipettes. *Biochemistry* **22**, 2319–2323.
- TAKEDA, K. & TRAUTMANN, A. (1984). A patch-clamp study of the partial agonist actions of tubocurarine on rat myotubes. *Journal of Physiology* **349**, 353–374.
- VAN DER KLOOT, W. G. & COHEN, J. S. (1979). Membrane surface potential changes may alter drug interactions: an example acetylcholine and curare. *Science* **203**, 1351–1353.

#### EXPLANATION OF PLATE

End-plate region of a living, enzyme-treated, muscle fibre as it is seen during an experiment. The upper photomicrograph shows the tip of a patch pipette placed on a synaptic trough. The nerve terminal is stripped off the muscle fibre. The shadow on the left is a glass hook which mechanically stabilizes the fibre. The lower micrograph shows the same fibre after incubating the preparation with rhodamine-labelled  $\alpha$ -bungarotoxin ( $2 \text{ mg ml}^{-1}$ , 2 h incubation), followed by fluorescence photography to show the distribution of ACh receptors. It is clearly seen that the tip of the pipette is within a few micrometres of the most densely stained region. Calibration is  $50 \mu\text{m}$ .